**Title: Florigen Activation Complex Dynamics and SVP-Mediated Repression Orchestrate Temperature-Regulated Flowering in Saffron**

**Authors:** Diksha Kalia[1, 2], Joel Jose-Santhi[1, 2], Firdous Rasool Sheikh[1, 2], and Rajesh Kumar Singh[1, 2, *]

**Affiliations:**

1. Plant Adaptation and Developmental Biology Lab, Department of Biotechnology, CSIR-Institute of Himalayan Bioresource Technology, Palampur, H.P., India-176061
2. Academy of Scientific and Innovative Research (AcSIR), Ghaziabad, 201002, India

**Author Details:**

Diksha Kalia, email: dikshakalia47@gmail.com,

Joel Jose-Santhi, email: joeljosesanthi@gmail.com,

Firdous Rasool Sheikh, email: sheikhfirdous191@gmail.com,

Rajesh Kumar Singh: *Corresponding Author, email: rajeshsingh@ihbt.res.in,

ORCID Id: 0000-0001-7831-7946

**Abstract**

Saffron, a high-value spice cultivated worldwide for its therapeutic and culinary uses, is a sterile triploid species, rendering conventional breeding approaches ineffective. This limitation underscores the need for molecular and biotechnological strategies for its genetic improvement. Flowering, a key determinant of saffron yield, is strongly influenced by temperature; however, the genetic regulatory networks underlying this process remain poorly understood. Our study identifies key regulators of saffron's flowering, focusing on the Florigen Activation Complex (FAC) components: *FLOWERING LOCUS T* (FT), bZIP transcription factor FD, and *TERMINAL FLOWER*-1 (TFL-1), and demonstrate their temperature-dependent roles in floral regulation. Spatiotemporal expression analyses suggested that *CsatFT3* and *CsatFD2*, expressed in the floral meristem promote floral induction, while *CsatTFL1*-3 acts as a floral repressor. Protein interaction studies showed that CsatFT3 and CsatTFL1-3 compete for binding to CsatFD2, and their balance modulates floral induction. Functional validation in Arabidopsis and Saffron confirmed these findings. Furthermore, we identified *CsatSVP2*, an ortholog of *SHORT VEGETATIVE PHASE* (SVP), as a low temperature-responsive repressor that directly binds the CsatFT3

promoter to inhibit its expression. Together, these findings enhance our understanding of temperature mediated floral induction in saffron and provide insights and lay the groundwork for genetic interventions to enhance yield under variable temperature conditions.

**Keywords:** Florigen activation complex (FAC), Flowering locus T(FT), bZIP transcription factor-FD, *TFL1*, Geophytes, Thermoresponsive, Thermoperiodic, Floral induction, Phosphatidyl Ethanolamine Binding Protein (PEBP), VIGS,

## Introduction

Saffron (*Crocus sativus* L.) is a sterile, clonally propagated, autotriploid geophytic monocot cultivated for its highly valued dried stigmas, which constitute the world's most expensive spice. While the stigmas are the primary edible and culinary component, other parts of the saffron plant also have diverse applications, including uses in agriculture, traditional medicine, and as a natural colouring agent, making the entire flower economically valuable (Ahrazem et al., 2015). Saffron has been predominantly cultivated for centuries in select regions such as Iran, India, Greece, Italy, Afghanistan, Morocco, Spain, and various Mediterranean basins (Cardone et al., 2020). Flowering is the key determinant of saffron's crop productivity, and this critical phase is increasingly influenced by environmental changes. As a thermoperiodic plant, saffron's flowering is primarily regulated by temperature. During the warm summer months, the transition from vegetative to reproductive growth occurs underground, with floral bud emergence only triggered by exposure to cooler temperatures (Molina et al., 2005a). This biphasic thermal requirement consists of an induction phase at warm temperatures lasting 50–150 days, followed by an emergence phase under cooler conditions, a pattern that has been well documented (Jose-Santhi et al., 2023; Molina et al., 2005a). The inappropriate temperature during the flowering transition leads to flower atrophy or no flower, causing yield loss (Wang et al., 2021). Saffron corms can sense the temperature change and modify the response accordingly (Molina et al., 2005b). Thus, there exists a thermoresponsive regulation of flowering in saffron which is still not well studied at the molecular level.

Flowering is a key transition in the angiosperm life cycle, marking the shift from vegetative to reproductive growth and representing a tightly regulated process vital for survival. This process is orchestrated by a complex network of environmental cues,

internal signalling pathways, hormonal regulation, and genetic programs that together ensure flowering occurs under optimal conditions (Zik and Irish, 2003). Key environmental pathways influencing flowering include photoperiod, ambient temperature, light quality, vernalization, and gibberellin signalling. These pathways operate in coordination with endogenous factors along with plant age and nutritional status, allowing plants to synchronize reproduction with favourable environmental windows (Andrés and Coupland, 2012; Freytes et al., 2021; Pyo et al., 2014; Srikanth and Schmid, 2011). Extensive studies in both monocot and dicot organisms, such as Arabidopsis thaliana and rice, have uncovered key regulatory components of flowering (Kinoshita and Richter, 2020). Central to this regulation are floral integrator genes, particularly *FLOWERING LOCUS T* (*FT*) in Arabidopsis and *Heading Date 3a* (*Hd3a*) in rice, which belong to the phosphatidylethanolamine-binding protein (PEBP) family. FT/Hd3a promotes flowering by forming the Florigen Activation Complex (FAC), composed of FD-like bZIP transcription factors and the florigen receptor 14-3-3 protein (Abe et al., 2005; Taoka et al., 2013). This complex activates floral meristem identity genes such as *LEAFY* and *APETALA1*, initiating floral development (Putterill et al., 2004; Simon et al., 1996; Wigge et al., 2005). In contrast, *TERMINAL FLOWER 1* (TFL1), another PEBP family member, acts antagonistically to repress flowering (Wickland and Hanzawa, 2015). In rice, Hd3a, RFT1, and OsFTL10 promote flowering by forming the Florigen Activation Complex (FAC) (Komiya et al., 2008; Tamaki et al., 2007). Conversely, OsFTL12, OsFTL4, RCN1, and RCN2 act as floral repressors by competing for FAC components to assemble a Florigen Repression Complex (FRC) (Nakagawa et al., 2002; Zheng et al., 2023). The dynamic balance between FAC and FRC finely regulates heading date and plant architecture in rice. Members of the FD family are key interaction partners of the PEBP family, playing roles in both promoting and repressing meristem differentiation, depending on their specific interacting partners (Zhu et al., 2020). Concurrently, the flowering program suppresses negative regulators, including *FLOWERING LOCUS C* (FLC), and *SHORT VEGETATIVE PHASE* (SVP), which are crucial for ensuring a proper transition from the vegetative to the reproductive phase mainly regulated by temperature (Bowman et al., 2012; Turck et al., 2008). Temperature-dependent flowering has been widely studied, with FT-like genes playing a central role (Capovilla et al., 2015). Upstream regulators include MADS-domain transcription factors such as SVP and FLC, which modulate flowering by forming complexes and repressing *FT* expression via direct binding to its

102 promoter (Balasubramanian et al., 2006; Gu et al., 2013; Lee et al., 2007). However,
103 the thermoresponsive pathway governing floral induction in saffron remains largely
104 unexplored.

105 In contrast to annuals, the regulation of flowering in perennial geophytes involves
106 modified or additional mechanisms to accommodate their extended life cycles, periods
107 of dormancy and dual reproduction (Khosa et al., 2021). This has been observed in
108 species like *Narcissus tazetta* (Noy-Porat et al., 2013), tulip (Tulipa spp.)
109 (Leeggangers et al., 2017a), and saffron (Molina et al., 2005a), where floral induction
110 occurs even in the absence of leaves. In these species, flowering is thought to be
111 mediated directly at the meristem level, independent of traditional photoperiod or
112 vernalization cues. Instead, ambient temperature plays a dominant role in determining
113 flowering time. These observations highlight the need to identify the specific genes
114 and mechanisms that govern flowering in geophytic perennials. Over evolutionary
115 time, the molecular mechanisms controlling flowering have grown increasingly
116 complex, involving intricate interactions between floral regulator genes and their
117 transcription factor partners, which form regulatory complexes (Wickland and
118 Hanzawa, 2015). Gene duplication and neofunctionalization have contributed to the
119 diversification of these regulatory genes. Both *FT* and *TFL1,* the central regulators of
120 flowering, have undergone gene duplication events in various lineages, leading to
121 paralogs with distinct functions that promote or inhibit flowering (Jin et al., 2021). This
122 evolutionary diversification is evident across many species. In geophytes, for instance,
123 members of the PEBP gene family have extended their functions beyond flowering to
124 include the formation of underground storage organs, contributing to both sexual and
125 asexual reproduction (Khosa et al., 2021). In species like potato, tulip, and others,
126 gene duplication has led to distinct roles in flowering, vegetative growth, and tuber or
127 bulb formation (Bellinazzo et al., 2025; Jing et al., 2023; Navarro et al., 2011). Similar
128 divergence has been observed in onion (*Allium cepa*), sugar beet (*Beta vulgaris*), and
129 hybrid aspen, demonstrating the complexity of flowering regulation in perennials (Hsu
130 et al., 2011; Lee et al., 2013b; Pin et al., 2010). Beyond the PEBP gene family,
131 functional diversification is seen in related pathways. In hybrid aspen, two FD
132 homologs, *FDL1* and *FDL2*, regulate seasonal growth differently (Tylewicz et al.,
133 2015). In rice, *OsFD2* contributes to leaf development while *OsFD1* regulates
134 flowering (Tsuji et al., 2013). FD-like transcription factors can have dual roles,

135 promoting or repressing flowering depending on their partners. For instance, *CmFDa*
136 in *Chrysanthemum morifolium* represses flowering through epigenetic regulation (Xue
137 et al., 2025). These examples highlight the evolutionary plasticity of flowering networks
138 and the importance of species-specific regulatory mechanisms.
139 Saffron, due to its sterile nature and extremely limited genetic diversity, is not
140 amenable to conventional breeding approaches, which hinders efforts to develop
141 climate-resilient, high-yielding, and stress-tolerant varieties. As a result, there have
142 been no significant advancements in improving saffron's adaptability to climate
143 change, making its cultivation increasingly vulnerable to environmental fluctuations.
144 Consequently, only biotechnological interventions can be employed to introduce
145 desirable traits. Despite its economic and agricultural importance, research on the
146 molecular regulation of flowering in saffron remains limited. Most existing studies have
147 focused on temperature effects on flowering physiology (Molina et al., 2005a; Wang
148 et al., 2021), and while several flowering-related genes have been identified through
149 transcriptomic and genomic analyses (Hu et al., 2020; Kalia et al., 2022; Renau-
150 Morata et al., 2021; Singh et al., 2023; Tsaftaris et al., 2013), these remain largely
151 descriptive and lack functional validation. Expression profiling has indicated the
152 involvement of multiple *FT* and *TFL1* homologs in saffron flowering (Kalia et al., 2022;
153 Renau-Morata et al., 2021; Tsaftaris et al., 2013), yet no functional characterization of
154 these genes has been reported. To fill this gap, we present a comprehensive
155 molecular framework for temperature-dependent floral induction in saffron, a
156 geophytic monocot with a unique flowering phenotype. By integrating gene expression
157 profiling, heterologous functional assays, protein–protein interaction studies, promoter
158 binding analyses, and virus-induced gene silencing, we identify key regulatory
159 components that mediate the floral transition in response to ambient temperature.
160 Overall, these findings advance our understanding of temperature-mediated flowering
161 in saffron and provide a foundation for genetic interventions aimed at improving yield
162 under fluctuating environmental conditions
163
164 **Methods**
165 **Plant materials and growth conditions**
166 Saffron corms *(Crocus sativus* L.) were grown under controlled conditions at CSIR-
167 IHBT, and samples were collected monthly from January to September, covering both
168 the vegetative growth and flowering phases (Jose-Santhi et al., 2023; Kalia et al.,

169 2022). To analyze gene expression patterns, apical buds, axillary buds, and corm
170 tissues were harvested across this period, with three biological replicates per time
171 point, each comprising pooled tissue from ten individual corms. For RT-qPCR
172 analysis, apical buds, axillary bud, corm tissue collected during the vegetative and
173 flowering stages were used, with detailed methods and results provided in the
174 Supplementary Information.
175 ViGS experiments were conducted using corms grown under the same controlled
176 conditions as described earlier. Corms with high flowering competency (weighing >10
177 g) were selected for the silencing of *CsatFT3* and *CsatFD2*. To investigate the role of
178 *CsatSVP2*, two experimental conditions were used: (i) standard growth conditions, and
179 (ii) a temperature-sensitive treatment in which corms were incubated at 8 °C during
180 the flowering phase to assess temperature-dependent gene regulation. For silencing
181 of *CsatTFL1-3/CEN1*, corms with lower flowering competency (weighing 7–9 g) were
182 utilized.
183 *Arabidopsis thaliana* (Col-0) was used as the wild-type background for transformation
184 experiments, and the ft1 mutant in the Ler background was used for functional
185 complementation of CsatFT3. *Nicotiana benthamiana* was used for transient
186 expression assays. Arabidopsis seeds were surface-sterilized with 4% sodium
187 hypochlorite and germinated on half-strength Murashige and Skoog (MS) medium. To
188 synchronize germination, seeds were stratified at 4°C for two days before being
189 transferred to a soil mixture of peat, vermiculite, and perlite (2:1:1). All plants were
190 cultivated in controlled growth chambers under long-day conditions (16 h light/8 h
191 dark) at 22°C for Arabidopsis and 25°C for *Nicotiana benthamiana*.
192
193 **RNA isolation and expression analysis by RT-qPCR**
194 Total RNA was isolated from saffron apical buds, axillary buds, corm tissues, and
195 Arabidopsis using the Plant Total RNA Isolation Kit (Sigma-Aldrich), according to the
196 manufacturer's protocol. For each sample, 1 µg of total RNA was used to synthesize
197 cDNA. Reverse transcription was performed using the RevertAid cDNA Synthesis Kit.
198 The transcript level of each gene was quantified by quantitative real-time PCR (q-PCR)
199 using gene-specific primers (Supplementary Table 1), generated by SnapGene
200 Viewer 5.3.1 software (version 0.4.0) using the System (BioRad CFX Opus Real time
201 PCR). Each expression analysis included three biological replicates, with each
202 replicate derived from pooled tissue of ten individual corms. RT-qPCR results are

203 presented as the mean ± standard error (SEM) of three technical replicates per
204 biological sample.
205
206 **Sequence alignments and phylogenetic analysis**
207 Protein sequences were aligned using the ClustalW algorithm with default parameters
208 to generate high-quality multiple sequence alignments. Visualization of the alignments
209 was performed using ESPript 3.x (Robert & Gouet, 2014) to highlight conserved
210 regions and structural features. The aligned sequences were exported in Newick
211 (.nwk) format for phylogenetic analysis. Phylogenetic tree construction was carried out
212 using the "build" function of ETE3 v3.1.3 (Huerta-Cepas et al., 2016), implemented via
213 the GenomeNet platform (https://www.genome.jp/tools/ete/). FastTree v2.1.8 (Price et
214 al., 2010) was used with default settings to infer approximately maximum-likelihood
215 phylogenetic trees.
216
217 **Plant transformation**
218 To generate Arabidopsis transgenic lines, full-length coding sequences (CDS) of the
219 target genes were amplified and first cloned into the pENTR entry vector using
220 Gateway® cloning technology. Subsequently, LR recombination was performed to
221 transfer the CDS into the destination vectors pK2GW7 (for overexpression analysis),
222 under the control of the Cauliflower Mosaic Virus (CaMV) 35S promoter. The resulting
223 constructs included 35S::*CsatFD1*, 35S::*CsatFD2*, 35S::*CsatFD3*, 35S::*CsatFT3*,
224 35S::*CsatTFL1-1*, 35S::*CsatTFL1-2*, 35S::*CsatTFL1-3*, 35S::*CsatSVP1*, and
225 35S::*CsatSVP2*. Primer sequences used for vector construction are provided in the
226 supplementary table 1 file. The final recombinant plasmids were introduced into
227 *Arabidopsis thaliana* (Col-0) via Agrobacterium tumefaciens strain GV3101 using the
228 floral dip transformation method. Transgenic seeds were harvested individually and
229 screened based on the appropriate selection marker. Homozygous T3 lines were
230 identified and used for further phenotypic characterization. Flowering time was
231 recorded as the number of days from germination to the emergence of the first floral
232 bud.
233
234 **Yeast one hybrid (Y1H) assay**
235 To examine the binding of CsatSVP2 to the CsatFT3 promoter, yeast one-hybrid (Y1H)
236 assays were conducted using the Matchmaker® Gold Yeast One-Hybrid System Kit

237 (Clontech). Promoter fragments of CsatFT3 containing the core CArG-box motif were
238 cloned into the pAbAi vector. The resulting recombinant pAbAi-promoter plasmids
239 were linearized with BstBI (NEB) and integrated into the genome of the Y1HGold yeast
240 strain. Transformants were selected on synthetic dextrose (SD) medium lacking uracil
241 (SD/-Ura). The coding sequence of CsatSVP2 was amplified and inserted into the
242 pGADT7-AD vector. The recombinant pGADT7-AD constructs were then introduced
243 into the Y1HGold strains containing the integrated CsatFT3 promoter. Protein–DNA
244 interaction was assessed by culturing the transformed yeast on SD medium lacking
245 leucine (SD/-Leu) and supplemented with Aureobasidin A (AbA) at a minimal inhibitory
246 concentration of 150 ng/mL for four days. Primer sequences used for cloning are
247 provided in Supplementary Table 1.
248
249 **Histochemical localization of GUS activity**
250 GUS activity was performed using the histochemical staining protocol described by
251 Jefferson (Jefferson et al., 1987). Transgenic *Arabidopsis thaliana* lines with
252 *ProCsatFT3::GUS* construct were incubated in a staining solution composed of 50 mM
253 sodium phosphate buffer (pH 7.2), 2.0 mM potassium ferricyanide [$K_3Fe(CN)_6$], 2.0
254 mM potassium ferrocyanide [$K_4Fe(CN)_6$], 0.1% (v/v) and 1.0 mg/mL X-Gluc (5-bromo-
255 4-chloro-3-indolyl-β-D-glucuronide). Samples were incubated at 37 °C for 5 hours to
256 allow GUS expression to develop. Following staining, tissues were cleared with 70%
257 (v/v) ethanol to remove chlorophyll and enhance contrast, then examined under a
258 stereo microscope (ZEISS Stemi 508). To validate GUS expression patterns, at least
259 ten independent transgenic lines were screened for the construct. Plants from three
260 confirmed GUS-positive lines were selected for detailed expression analysis at various
261 developmental stages, including 7, 14, and 21 days after germination (DAG),
262 inflorescence emergence, flowering, and silique formation. For the flowering and
263 silique stages, staining was performed on aerial tissues from soil-grown plants
264
265 **Yeast two-hybrid (Y2H) assays**
266 Yeast two-hybrid assays were conducted following the manufacturer's protocol using
267 the Matchmaker™ Two-Hybrid System (Clontech). The coding sequences of
268 CsatFD1, CsatFD2, and CsatFD3 were cloned into the bait vector pGBKT7, whereas
269 those of CsatFT3, CsatTFL1-1, CsatTFL1-2, and CsatTFL1-3 were inserted into the
270 prey vector pGADT7. The primers used for amplification are provided below. Bait and

271 prey plasmids were co-transformed into the Y2HGold yeast strain and cultured on
272 synthetic dextrose (SD) medium lacking tryptophan (SD/-Trp) and leucine (SD/-Leu)
273 for 3–5 days at 30°C. Protein-protein interactions were assessed by selecting colonies
274 on SD medium lacking Trp, Leu, and histidine (SD/-Trp/-Leu/-His).
275
276
277 **Bimolecular fluorescence complementation (BiFC)**
278 The coding sequences of *CsatFD1*, *CsatFD2*, *CsatFD3* Cloned into YFP C-terminal
279 (YFPC) and *CsatFT3*, *CsatTFL1-1*, *CsatTFL1-2*, *CsatTFL1-3* were cloned into the
280 YFP N-terminal (YFPN) vectors. Primer sequences used for vector construction are
281 provided in the supplementary table 1. These constructs were then introduced into
282 Agrobacterium tumefaciens strain GV3101 for transient expression in 5-week-old
283 *Nicotiana benthamiana* leaves. After co-infiltration for 48 hours, fluorescence was
284 imaged using a confocal laser scanning microscope (Leica, Stellaris 5, Germany). YFP
285 fluorescence was excited at 514 nm, with emission detected between 522 and 560
286 nm.
287
288 **Firefly Complementation Assay**
289 The full-length coding sequences (CDSs) of CsatFT3, CsatTFL1-3, and CsatFD2 were
290 cloned into the pCAMBIA1300-nLUC and pCAMBIA1300-cLUC vectors, respectively,
291 and introduced into Agrobacterium tumefaciens strain GV3101. Various combinations
292 were co-infiltrated into Nicotiana benthamiana leaves. The infiltrated plants were
293 incubated at 22 °C for two days. Prior to LUC activity detection, the leaves were
294 sprayed with 1 mM D-luciferin (Potassium Salt, BioVision) and incubated in the dark
295 for 8 minutes to eliminate background fluorescence. Fluorescence was detected using
296 a cooled CCD camera system (Bio-Rad Chemi Doc). Relative LUC intensity was
297 quantified using ImageJ software. Statistical analysis was performed using one-way
298 ANOVA, and significance was assessed using the Compact Letter Display (CLD)
299 method to indicate differences at a significant p-value level. Primer sequences used
300 in these assays are provided in Supplementary Table 1.
301
302 **Genome walker library for promoter amplification**
303 The 5′ upstream region of the CsatFT3 gene from Crocus sativus was obtained using
304 the Genome Walker™ kit (Clontech, USA). Genomic DNA was extracted from leaf

305 tissue following the protocol provided with the QIAGEN DNA isolation kit, then
306 digested with two blunt-end restriction enzymes, DraI and EcoRV, and further ligated
307 with adapters, to generate Genome Walker libraries. Gene-specific primers (GSPs),
308 designed based on the CsatFT3 cDNA sequence, were used alongside adaptor
309 primers from the kit to carry out primary and nested PCR amplifications as listed in
310 Supplementary Table 1. The amplified PCR products were resolved on a 1% (w/v)
311 agarose gel, purified, and cloned into the pGEM-T Easy vector (Promega, USA) for
312 sequencing. The resulting CsatFT3 promoter sequence was analyzed using the
313 PlantCARE database (Lescot et al., 2002) to identify potential cis-regulatory elements
314 involved in transcriptional regulation.
315

316 **Virus-induced gene silencing (VIGS)**

317 Virus-induced gene silencing (VIGS) was carried out following the protocol established
318 in lab (Kalia et al., 2024). Gene-specific fragments were amplified for *CsatFT3* (300
319 bp, flanked by EcoRI sites), *CsatFD2* (292 bp, flanked by BamHI sites), *CsatTFL1-3*
320 (302 bp, containing both EcoRI and BamHI sites), and *CsatSVP2* (318 bp, with
321 EcoR1and BamH1 sites) restriction sites at both termini. These fragments were cloned
322 into the pTRV2 vector to generate the constructs. Agrobacterium-mediated infiltration
323 was performed as previously described (Kalia et al., 2024). To confirm gene silencing,
324 transcript levels of *CsatFT3*, *CsatFD2*, *CsatTFL1-3*, and *CsatSVP2* were quantified by
325 RT-qPCR in apical buds collected at the floral induction stage. Phenotypic analysis of
326 flower development was conducted when floral buds reached the floral emergence
327 stage. Primer sequences used for the VIGS assay are listed in Supplementary table
328 1.
329

330 **Luciferase assay**

331 To investigate the regulatory effect of *CsatSVP2* on the *CsatFT3* promoter, a
332 luciferase reporter assay was conducted in *Nicotiana benthamiana* leaves. Promoter
333 sequences of *CsatFT3* were cloned into the Gateway-compatible vector pGWB435
334 (Invitrogen) upstream of the luciferase (Luc) reporter gene. Three promoter constructs
335 were generated: (i) the full-length promoter (FL), (ii) a truncated fragment containing
336 the CArG motif(T1), and (iii) a truncated fragment lacking the CArG motif (T2). The
337 *CsatSVP2* coding sequence was separately cloned into pGWB402 under the control
338 of the CaMV35S promoter to serve as an effector. Control treatments included empty

339 vectors (pGWB435 and pGWB402) as a negative control, and *ProCsatFT3*::Luc alone
340 as a positive control. Constructs were introduced into the *Agrobacterium tumefaciens*
341 strain GV3101 and co-infiltrated into *Nicotiana benthamiana* leaves. Each leaf was
342 divided into four quadrants to enable side-by-side comparisons of different treatments
343 within the same biological context. Luciferase activity was visualized and quantified
344 using ImageJ software. The experiment was repeated independently at least three
345 times in separate leaves to ensure reproducibility. One-way ANOVA was used for
346 statistical analysis, and differences among treatments were determined using
347 Compact Letter Display (CLD) to indicate statistically significant differences ($p < 0.05$).
348

349 **Statistical analyses**

350 All statistical analyses were conducted using GraphPad Prism version 10 for Windows
351 (GraphPad Software, Boston, MA, USA; www.graphpad.com). One-way ANOVA
352 followed by Tukey's Honest Significant Difference (HSD) test was applied for multiple
353 comparisons. Statistically significant differences between groups at $p < 0.05$ are
354 indicated by different letters, as determined by Compact Letter Display (CLD). Two-
355 way ANOVA to assess the effects of temperature, month, and their interaction,
356 followed by Sidak's multiple comparisons test and Student's t-test for one-to-one
357 comparison. (*: $p<0.05$; **: $p<0.01$***: $p<0.001$) (****: $p<0.0001$).
358

359 **Results:**

360 **CsatFT3 functions as a temperature-sensitive regulator of floral induction in**
361 **saffron**

362 Our previous work identified several PEBP family genes implicated in flowering
363 regulation in saffron, with *CsatFT3* emerging as a potential key regulator of floral
364 induction (Kalia et al., 2023). However, that study was limited to spatial and temporal
365 expression profiling during the reproductive phase transition. To further elucidate the
366 functional role of *CsatFT3*, we investigated its expression dynamics across vegetative
367 and reproductive phases in saffron apical buds. We found that *CsatFT3* is specifically
368 expressed during the reproductive phase, with transcript accumulation coinciding with
369 the floral induction stage (Figure 1A, Supplementary Figure 1). In contrast, its
370 expression was barely detectable in apices of newly developing corms and during the
371 vegetative phase in winter. Given that low temperatures are known to suppress floral
372 induction in saffron (Jose-Santhi et al., 2023), we next assessed *CsatFT3* expression

373 in apical buds of corms stored under low (8°C) and ambient (25°C) temperature
374 conditions following the vegetative phase. Consistent with a temperature-responsive
375 role, *CsatFT3* transcript levels were markedly reduced in corms stored at 8°C
376 compared to those maintained at 25°C (Figure 1B).
377 To further investigate tissue- and temperature-specific expression of the *CsatFT3*
378 gene, we isolated a 1.2 kb fragment of the *CsatFT3* promoter (Supplementary figure
379 2) that contains several core, distal, and proximal promoter elements and constructed
380 a promoter-GUS fusion construct. GUS-driven transcription reporter lines of *CsatFT3*
381 displayed meristem and flower-specific expression in Arabidopsis, consistent with our
382 spatiotemporal expression profiling in saffron (Figure 1C and Supplementary figure 3).
383 Furthermore, these *ProCsatFT3::GUS* fusion lines demonstrated temperature-
384 sensitive regulation, with expression gradually decreasing as the temperature was
385 lowered, in line with our previous findings that low temperatures suppress the
386 expression of *CsatFT3* (Figure 1D). At low temperatures (4°C), GUS activity was
387 nearly undetectable, indicating a significant suppression of expression under cold
388 conditions. These findings reinforce the role of *CsatFT3* in temperature-sensitive
389 flowering regulation in saffron and suggest that its expression is activated under the
390 relatively high-temperature conditions that promote floral induction.
391 To functionally validate the role of *CsatFT3* in floral regulation, we ectopically
392 expressed *CsatFT3* in Arabidopsis Col-0 and complemented the late-flowering *ft-1*
393 mutant (Ler-0). Overexpression in Col-0 resulted in a significant early-flowering
394 phenotype (Figure 1E–G), while *ft-1* plants transformed with *CsatFT3* exhibited
395 restored or even earlier flowering compared to wild-type (Figure 1H–J). These results
396 confirm that *CsatFT3* is functionally conserved and capable of promoting flowering in
397 a heterologous system. Following confirmation of CsatFT3's involvement in floral
398 induction and flowering, finally, to evaluate the role of *CsatFT3* in its native we
399 performed Virus-Induced Gene Silencing (VIGS) of *CsatFT3* in saffron corms and
400 monitored flowering. Silencing of *CsatFT3* led to a significant reduction in its transcript
401 levels in apical buds (Figure 1K) and was accompanied by a marked decrease in
402 flowering percentage compared to TRV2 mock-infected controls (Figure 1L–M). No
403 significant decrease of *CsatFT1* and *CsatFT2* was observed in TRV2-silenced
404 CsatFT3 corms (Supplementary Figure 4). Together, these findings establish CsatFT3
405 as a temperature-sensitive floral inducer in saffron, functioning as a key regulatory
406 component during the transition from vegetative to reproductive growth.

407

408 **Identification of florigen activation complex component FD, involved in**
409 **flowering induction in saffron**

410 *FT* like genes requires interaction with bZIP transcription factor-*FD* to form FT-FD
411 complex that directly activates the floral meristem identity genes. Thus, to identify the
412 FD like genes involved in floral induction of saffron we have cloned full length cDNAs
413 for three FD-like genes (*CsatFD1*, *CsatFD2* and *CsatFD3*), which encodes for 197,
414 215 and 245 aa of proteins respectively. All the three FDs are similar to FD proteins
415 from other plants and contains the conserved basic region, Leucine zipper region and
416 the functionally important conserved threonine (T)/SAP motif at the C terminus
417 (Supplementary Figure 5A). Phylogeny aligns CsatFD's with monocot FDs with
418 Asparagus officinalis as the nearest family member (Supplementary Figure 5B).

419 We next investigated the expression profiles of the three saffron *FD* genes during the
420 vegetative and flowering induction stages. Interestingly, the expression of *CsatFD2*
421 coincided with the floral induction stage, whereas *CsatFD3* showed higher expression
422 at later stages of sprouting, specifically in July, when floral differentiation and
423 vegetative growth begin (Figure 2 A). In contrast, *CsatFD1* was expressed at relatively
424 stable levels throughout flower initiation and the vegetative phase, but its expression
425 was generally lower compared to *CsatFD2* and *CsatFD3*. In saffron, the apical bud
426 gives rise to the flower, while the axillary buds contribute only to vegetative growth,
427 thereby distinguishing the reproductive meristem from the vegetative meristems (Kalia
428 et al., 2022). Notably, *CsatFD2* was predominantly expressed in apical buds and
429 flower tissues, indicating a primary role in flowering (Figure 2B, C). Additionally,
430 *CsatFD2* showed comparatively higher expression in flower tissues compared to the
431 other two FD genes (Figure 2C). We also examined the temperature-sensitive
432 expression of these genes in corms stored at low (8°C) and ambient high (25°C)
433 temperatures. Our results revealed that CsatFD2 expression was significantly
434 downregulated at low temperatures (Figure 2D), whereas CsatFD1 and CsatFD3 did
435 not show a similar trend (Supplementary Figure 6A). Notably, CsatFD1 expression
436 remained unchanged at 8°C in June, the period when floral induction typically occurs.
437 Interestingly, CsatFD3 showed higher expression in corms stored at low temperatures
438 compared to those stored at 25°C (Supplementary Figure 6B).

439 Next, we examined the effect of ectopic expression of the saffron *FD* genes in
440 Arabidopsis. Ectopic expression of *CsatFD2* can only induce early flowering in

441 Arabidopsis, whereas there was no significant phenotypic change observed in
442 *CsatFD1* and *CsatFD3* expressing Arabidopsis plants (Figure 2E). These findings
443 were further supported by measurements of days to flowering and the number of
444 rosette leaves in the Arabidopsis transformants (Figures 2F-K). These results further
445 suggest that *CsatFD2* may be the primary gene involved in flowering regulation in
446 saffron. To confirm the role of *CsatFD2* during floral induction, we silenced the gene
447 using Virus-Induced Gene Silencing (VIGS) in flower-competent saffron corms.
448 Compared to the TRV2 control, silencing of *CsatFD2* resulted in a reduction in flower
449 formation and overall flowering percentage (Figure 2L). VIGS silencing of CsatFD2
450 also led to a significant decrease in its transcript levels (Figure 2M), but did not affect
451 the expression of *CsatFD1* and *CsatFD3* (Supplementary Figure 7 A and B). These
452 results suggest that *CsatFD2* is a key component of the Floral Activator Complex
453 (FAC) involved in floral induction in saffron.
454
455 **TFL1-3/CEN1 is a newly identified negative regulator of flowering induction in**
456 **saffron**
457 In our previous study (Kalia et al., 2023), we identified two homologs of *TFL-1*/*CEN*,
458 named Csat*TFL1-1* and Csat*TFL1-2*, and through spatio-temporal expression
459 profiling, we proposed that TFL1-2 may play a role in determining flowering
460 competency in saffron (Supplementary figure 8A and B). However, neither of these
461 two *TFL-1* genes exhibited a temperature-sensitive response (Supplementary Figure
462 9A and B). Furthermore, ectopic expression of *CsatTFL1-1* and *CsatTFL1-2* in
463 Arabidopsis led to delayed bolting in only *CsatTFL1-2* plants compared to wild-type
464 (WT) under long-day (LD) conditions, whereas *CsatTFL1-1* transformants bolted
465 normally, similar to WT plants (Supplementary figure 10A-F). Additionally, interaction
466 studies, including BiFC and Y2H assays, did not reveal any positive interactions with
467 *CsatFD2*, our identified positive regulator of flowering (Supplementary Figure 11A and
468 B). These findings prompted us to investigate further, hypothesizing that another
469 homolog of TFL1/CEN might be involved in floral induction in saffron. Through corm
470 development studies in our lab (Jose-Santhi et al., 2023), we identified a third *TFL1*
471 homolog, which exhibited higher expression during the vegetative phase. This gene
472 shares similarities with *CsatTFL1-1* and *CsatTFL1-2*, but phylogenetic analysis
473 clustered it within the CEN subgroup. Based on this, we named it *CsatTFL1-3*/*CEN1*
474 (Supplementary Figure 12A and B). Like other TFL1/CEN family members, TFL1-

475 3/CEN1 contains the conserved domains characteristic of this gene family.
476 Quantitative PCR (qPCR) expression profiling revealed that *CsatTFL1-3*/*CEN1*
477 expression is elevated during the vegetative phase, with a significant decrease during
478 the reproductive phase (Figure 3A). Tissue-specific expression analysis confirmed
479 that *CsatTFL1-3*/*CEN1* is predominantly expressed in the axillary bud tissue, further
480 supporting its potential role in negatively regulating flowering (Figure 3 C and D).
481 Next, we examined the expression of *CsatTFL1-3*/*CEN1* in corms stored at low (8°C)
482 and ambient (25°C) temperatures. Interestingly, there was no reduction in *TFL1-*
483 *3*/*CEN1* expression in corms stored at low temperatures compared to those stored at
484 ambient high temperatures, suggesting that it may be regulated by temperature and
485 could play a role in temperature-mediated floral induction in saffron (Figure 3B). We
486 then performed ectopic expression of *CsatTFL1-3*/*CEN1* in *Arabidopsis thaliana* (Col-
487 0) under the control of the constitutive 35S promoter. Transgenic lines exhibited a
488 significant delay in flowering compared to wild-type plants, as evidenced by increased
489 days to bolting and a higher number of rosette leaves at flowering (Figure 3F-G).
490 These results confirm the ability of TFL1-3/CEN1 to act as a floral repressor in
491 Arabidopsis, consistent with its proposed function in saffron. Notably, ectopic
492 expression of TFL1-3/CEN1 also led to a hyper-vegetative shoot phenotype,
493 characterized by the development of an inflorescence composed of leaf primordia
494 surrounded by small, serrated leaves—a phenotype not observed in TFL1-1 or TFL1-
495 2 expressing Arabidopsis lines (Figure 3E). Finally, we performed Virus-Induced Gene
496 Silencing (VIGS) of *CsatTFL1-3*/*CEN1* in low-flower-competent saffron corms. In
497 comparison to TRV2 control plants, silencing of *CsatTFL1-3*/*CEN1* led to the formation
498 of floral structures in 7-9 g corms (classified as low-flower-competent), and these
499 flowers appeared earlier than in TRV2 controls (Figure 3G-I). Importantly, VIGS of
500 *CsatTFL1-3*/*CEN1* did not affect the transcript levels of the other two *TFL1* homologs,
501 TFL1-1 and TFL1-2 (Supplementary Figure 13 A and B), suggesting TFL1-3/CEN1
502 and not TFL1-1 or TFL1-2 could play a role in flowering in saffron. This observation
503 suggests that TFL1-3/CEN1 acts as a negative regulator of floral induction, and its
504 silencing promotes floral transition in otherwise low-flowering competence corms.
505

506 **The FT-FD-TFL complex involved in floral regulation**

507 Our earlier analyses identified *CsatFT3*, *CsatFD2*, and *CsatTFL1-3*/*CEN1* as potential
508 core components of a Floral Activator Complex (FAC) in saffron. To investigate

509 whether these proteins physically interact to form functional regulatory complexes,
510 we employed two complementary approaches: yeast two-hybrid (Y2H) assays and
511 bimolecular fluorescence complementation (BiFC) in *Nicotiana benthamiana*. In the
512 Y2H assays, the coding sequences (CDS) of the three *CsatFD* genes were cloned into
513 the pGADT7 prey vector, and co-transformed into yeast with either *CsatFT3* or
514 *CsatTFL1-3*/*CEN1* fused to the pGBKT7 bait vector. Interaction screening revealed
515 that both CsatFT3 and TFL1-3/CEN1 specifically interacted with CsatFD2, but not with
516 CsatFD1 or CsatFD3 (Figure 4 A and B). These results suggest that CsatFD2 may
517 serve as a central interacting hub for both activator (FT3) and repressor (TFL1-3)
518 proteins within the FAC.
519 We further validated these interactions by BiFC assays in *Nicotiana benthamiana*
520 leaves. YFP fluorescence was observed in nuclei of cells co-expressing the C-terminal
521 half of YFP fused to CsatFD2 (cYFP–CsatFD2) with the N-terminal half of YFP fused
522 to either CsatFT3 (nYFP–CsatFT3) or CsatTFL1-3 (nYFP–CsatTFL1-3) (Figure 4 C
523 and D). No YFP fluorescence was detected in negative controls, including co-
524 expression of cYFP–CsatFD2 with nYFP alone or cYFP alone with nYFP–CsatFT3 or
525 CsatTFL1-3. Furthermore, consistent with the Y2H results, no BiFC signal was
526 observed when CsatFT3 or TFL1-3/CEN1 were co-expressed with CsatFD1 or
527 CsatFD3 (Supplementary Figure). Together, these findings strongly support a model
528 in which CsatFD2 specifically interacts with both CsatFT3 and TFL1-3/CEN1,
529 suggesting that competitive complex formation may modulate floral transition in
530 saffron.
531 Given the antagonistic roles of CsatFT3 and CsatTFL1-3 in the regulation of flowering,
532 and their respective interactions with the transcription factor CsatFD2, it was
533 hypothesized that CsatFT3 and CsatTFL1-3 may compete for binding to CsatFD2. To
534 investigate this, a luciferase complementation imaging (LCI) assay was conducted in
535 *Nicotiana benthamiana* leaves to evaluate the interaction strength between CsatFD2-
536 nLUC and cLUC-CsatTFL1-3 in the presence or absence of SK-CsatFT3.Strong
537 luciferase (LUC) activity was observed when CsatFD2-nLUC and cLUC-CsatTFL1-3
538 were coexpressed, indicating a robust interaction. However, coexpression with SK-
539 CsatFT3 significantly reduced LUC activity, suggesting that CsatFT3 interferes with
540 the interaction between CsatTFL1-3 and CsatFD2. Moreover, this suppression was
541 dose-dependent, with increasing amounts of CsatFT3 leading to a progressive
542 decrease in LUC signal (Figure 4E). Biological replicates supporting these

observations are presented in Supplementary figure 15 A and B. These results strongly suggest that CsatFT3 competes with CsatTFL1-3 for interaction with CsatFD2, which interferes with CsatTFL1-3's ability to interact with CsatFD2.

**CsatSVP2 Acts Upstream of FT3 in Temperature-Mediated Floral Repression**

To identify upstream genes potentially involved in temperature-dependent floral induction in saffron, we screened transcriptome data representing the suppression of floral induction under low temperatures (Jose-Santhi et al., 2023) and identified two partial SVP-like MADS-box genes that were upregulated in non-flowering samples. SVP-like genes are known to regulate flowering in a temperature-dependent manner (Lee et al., 2007). Using long-read and other in-house transcriptome data, and based on sequence similarity, we obtained full-length sequences of these two SVP-like genes. We isolated and cloned them from saffron, naming them *CsatSVP1* and *CsatSVP2*. Sequence analysis indicated that while these genes are highly similar, they code for different amino acid sequences. Multiple sequence alignment revealed that both CsatSVP1 and CsatSVP2 contain the conserved MADS-box domain, and phylogenetic analysis grouped them with SVP-like genes from other geophytes, such as Narcissus, Zingiber, and Lilium (Supplementary Figure 16 A and B).

To further characterize their role in flowering, we performed expression analysis of *CsatSVP1* and *CsatSVP2* during vegetative and floral induction stages. Both genes showed a significant reduction in expression during the floral induction stage (June); however, the reduction in *CsatSVP2* was more pronounced and correlated closely with floral induction and subsequent stages (Figure 5A). We then evaluated their expression in corms stored under floral inductive (25°C) and non-inductive (8°C) conditions. *CsatSVP2* transcript levels remained high at both temperatures, suggesting it may contribute to the floral repression observed at low temperatures (Figure 5C). In contrast, *CsatSVP1* expression decreased under both conditions, showing no temperature-dependent pattern (Figure 5B). Additionally, *CsatSVP2* expression was comparatively higher in floral tissues than *CsatSVP1*, further supporting its potential regulatory role (Supplementary Figure 17).

Next, to functionally validate these genes, we ectopically expressed both *CsatSVP1* and *CsatSVP2* in Arabidopsis under a constitutive promoter. Ectopic expression of both genes resulted in delayed flowering, with a more pronounced delay in the CsatSVP2-transformed lines compared to both the control and *CsatSVP1* lines (Figure

577 5D-I). Arabidopsis plants expressing *CsatSVP2* displayed various phenotypic changes
578 in flower bud and flower morphology, producing smaller, more compact flowers and
579 shorter siliques (Supplementary Figure 18). To investigate the role of *SVP* in
580 temperature-mediated floral suppression, we silenced *CsatSVP2* in saffron corms
581 using Virus-Induced Gene Silencing (VIGS). Csat*SVP2* was selected due to its
582 expression pattern and phenotype in Arabidopsis, which correlated with its expected
583 function. Since low temperatures during storage or dormancy are known to suppress
584 flowering, and CsatSVP2 may be involved in this process, we stored the *CsatSVP2*-
585 silenced corms at low temperatures, alongside a mock control (TRV2). Silencing of
586 SVP2 resulted in flowering in corms at low temperatures, whereas the TRV2-treated
587 corms stored at low temperatures did not flower (Figure 5J). In parallel, corms stored
588 at 25°C—an inductive condition—showed flowering in both control and SVP2-silenced
589 groups, confirming that *CsatSVP2* acts specifically in the floral suppression
590 mechanism under cold conditions (Figure 5K). Gene expression analysis further
591 revealed that *CsatSVP2* silencing prevented the typical low-temperature-mediated
592 suppression of *CsatFT3* expression, thereby facilitating flowering (Figure 5P and Q).
593 These findings suggest that CsatSVP2 and CsatFT3 act within the same regulatory
594 pathway, mediating temperature-responsive floral induction in saffron.
595
596 **SVP2 Directly Binds to the CsatFT3 Promoter and Represses Its Expression**
597 Our previous results indicated that CsatSVP2 and CsatFT3 function in the same
598 temperature-sensitive regulatory pathway: low temperature maintains or upregulates
599 CsatSVP2 expression, which in turn suppresses *CsatFT3*, thereby repressing floral
600 induction. Notably, *CsatFT3* transcript levels were restored in *CsatSVP2*-silenced
601 corms, suggesting that CsatSVP2 functions upstream of *CsatFT3*. To further explore
602 the mechanism of this regulation, we analyzed the CsatFT3 promoter sequence to
603 identify potential binding motifs for MADS-box transcription factors. In silico analysis
604 of the 1.2 kb FT3 promoter, previously shown to drive temperature-responsive
605 expression, revealed a conserved CArG-box motif (CCATTTAAGG) located
606 approximately 827 bp upstream of the ATG start codon that is established for binding
607 of MADS boxes genes including SVP orthologs (Figure 6A). To experimentally test
608 further whether CsatSVP2 directly binds to the *CsatFT3* promoter, we performed a
609 yeast one-hybrid (Y1H) assay. The Y1H assay confirmed that CsatSVP2 specifically
610 binds to the *CsatFT3* promoter, supporting the hypothesis of direct regulation (Figure

611 6B). To further validate the functional specificity of this interaction, we employed a
612 luciferase reporter assay using *Nicotiana benthamiana* transient expression (Figure
613 6C) and conducted a luciferase reporter assay using three different FT3 promoter
614 fragments: (1) the full-length promoter (~1.2kb), (2) a truncated version containing the
615 conserved CArG motif (T1), and (3) a truncated version lacking the motif (T2) (Figure
616 6D). Co-expression of CsatSVP2 with these constructs in *Nicotiana benthamiana*
617 revealed that luciferase activity was significantly reduced in both the full-length and T1
618 constructs (Figure6 D and F). In contrast, no repression was observed with the T2
619 construct, confirming that SVP2 specifically suppresses FT3 expression through direct
620 binding to the CArG motif (Figure 6F). Together, these results establish a mechanistic
621 model in which CsatSVP2 acts as a temperature-responsive floral repressor that
622 directly binds to the FT3 promoter via a conserved CArG motif, thereby repressing
623 FT3 expression and floral induction under low-temperature conditions.
624

625 **Discussion**

626 Saffron is a high-value crop cultivated in limited regions due to its strict temperature
627 requirements, which distinctly regulate its vegetative and reproductive growth. High
628 temperatures induce flowering, while subsequent cooling triggers flower formation. In
629 contrast, low temperatures suppress floral induction and support vegetative growth,
630 enabling overwintering and daughter corm development (Molina et al., 2005a). This
631 temperature sensitivity restricts saffron cultivation to specific climates. Although
632 environmental control of flowering has enabled cultivation in soilless and controlled
633 settings, the molecular mechanisms underlying temperature-regulated flowering
634 remain poorly understood. As a sterile crop, saffron cannot be improved through
635 conventional breeding, making biotechnological interventions essential. However,
636 limited genomic and genetic resources, challenges in genetic transformation, and a
637 scarcity of molecular studies have hindered progress in functional genomics, creating
638 a critical knowledge gap that must be addressed.

639 In this study, we have identified a temperature-sensitive transcriptional network that
640 regulates flowering in saffron, uncovering both conserved and saffron-specific
641 components involved in floral induction (Figure 7). Our data establish a regulatory
642 module involving CsatFT3, CsatFD2, CsatTFL1-3/CEN1, and CsatSVP2 as key
643 components in mediating floral transition in response to temperature cues. Although
644 the core elements of the Florigen Activation Complex (FAC) - FT, FD, and TFL1 are

645 conserved across angiosperms, their expression patterns, protein interactions, and
646 functional dynamics in saffron suggest neofunctionalization in line with its geophytic
647 lifecycle. For instance, Notably, CsatFT3 and CsatFD2 are upregulated at higher
648 temperatures and co-expressed in the floral meristem, promoting flowering. In
649 contrast, other FT and FD homologs show no such expression correlation (Figure 2;
650 (Kalia et al., 2022), indicating their limited or no involvement in floral induction.
651 Similarly, CsatTFL1-3 functions as a floral repressor by competitively binding to
652 CsatFD2, whereas the other two TFL1 homologs neither interact with CsatFD2 nor
653 delay flowering in Arabidopsis, suggesting a lack of functional redundancy and
654 functional specificity. Functional validation in both Arabidopsis and saffron confirms
655 that floral induction is governed by the dynamic interplay between CsatFT3, CsatFD2,
656 and CsatTFL1-3.Given the roles of gene duplication, neofunctionalization, and
657 lineage-specific gene expansion in driving the specialization of reproductive and
658 vegetative pathways in geophytes (Khosa et al., 2021), our identification of distinct
659 regulatory factors and their molecular interactors from multigene families in saffron
660 represents a significant advance.
661 A distinguishing feature of floral induction observed in saffron is the spatial restriction
662 of flowering-related gene expression predominantly to the meristem. All the genes
663 identified in this study were specifically expressed in the apical (flowering) meristem.
664 During floral induction, saffron corms are either underground or stored in the dark and
665 remain leafless, indicating that the molecular signals initiating flowering are localized
666 within the apical buds. Such meristem-localized control may reflect an adaptation to
667 the geophytic habit of saffron, which undergoes floral induction in the absence of
668 foliage, similar to what has been observed in other geophytes such as tulips
669 (Leeggangers et al., 2017a). This localization supports the hypothesis that
670 temperature cues are sensed and interpreted locally within the corm, rather than
671 systemically via leaves, as observed in many other species, including some geophytes
672 (Lee et al., 2013b; Navarro et al., 2011; Wigge, 2011; Wu et al., 2022; Yan et al.,
673 2021).
674 Temperature plays a pivotal role in regulating flowering time across plant species,
675 often through conserved thermosensory pathways. In Arabidopsis, warmer
676 temperatures promote flowering via *FT* activation (Balasubramanian et al., 2006).
677 while in crops like strawberry and onion, cold exposure induces flowering by triggering
678 FT-like genes (Heide, 1977; Lee et al., 2013b). Interestingly, the effect of temperature

679 on flowering is not always straightforward. Temperatures above 25°C seem to have
680 both inductive and repressive effects on flowering, depending on the species and
681 environmental conditions (Nakano et al., 2013; Noy-Porat et al., 2013; Oda et al.,
682 2012). This temperature sensitivity is closely linked to the regulation of FT, a key gene
683 that integrates various environmental signals and controls the timing of flowering. In
684 *Narcissus tazetta* (daffodils), floral induction is triggered by high ambient temperatures
685 (25°C) through the activation of *NtFT*, while in tulips, *TgTFL1* downregulation and
686 *TgFT2* upregulation contribute to temperature-induced floral induction (Leeggangers
687 et al., 2017b; Noy-Porat et al., 2013). In contrast, in species like onion and lily, which
688 flower in spring, vernalization (low-temperature treatment) is required to activate the
689 expression of *AcFT2* and *LiFT*, respectively (Lee et al., 2013b). In our study, we also
690 found that *CsatFT3*, a key flowering-time gene in saffron, is temperature-regulated,
691 with its expression being induced by high ambient temperatures and suppressed by
692 low temperatures (Figure 1B). Similarly, *CsatFD2*, a partner of *CsatFT3* in the
693 flowering regulatory network, follows a similar expression pattern, suggesting their
694 involvement in the temperature-mediated floral induction pathway in saffron.
695 Interestingly, we observed that *CsatTFL1-3*, a gene that maintains the vegetative state
696 and prevents early flowering, exhibits a reciprocal expression pattern. In Arabidopsis
697 low and ambient temperature regulation of flowering involves the gene *TFL1* (Strasser
698 et al., 2009). Higher expression of *CsatTFL1-3* is observed during the vegetative
699 phase, which coincides with the low winter temperatures during saffron's growth cycle
700 (Figure 3A). This expression pattern is crucial for maintaining the vegetative phase
701 and delaying flowering, as confirmed by the hyper-vegetative shoot phenotype in
702 *TFL1*-3 overexpressing Arabidopsis plants (Figure 3) similar to what was observed
703 when Arabidopsis *TFL1* is overexpressed (Lee et al., 2019). In contrast, as
704 temperatures rise in the summer, the expression of CsatFT3 increases (Figure 1A),
705 likely triggering the activation of floral pathway genes and the transition to reproductive
706 development. Overall, a balance between CsatFT3, CsatTFL1-3, and their interaction
707 with CsatFD2 governs floral induction in a temperature-dependent manner. This
708 delicate interplay between temperature and gene expression is vital for ensuring
709 proper timing of flowering in saffron, aligning the plant's reproductive phase with
710 favourable environmental conditions.
711 We also identify CsatSVP2, a MADS-box transcription factor, as a critical floral
712 repressor acting upstream of FT–FD–TFL core module. MADS-box genes are key

713 regulators of flowering time, with SVP-like genes playing central roles in ambient
714 temperature-mediated floral control (Jin and Ahn, 2021). CsatSVP2 directly binds a
715 conserved CArG-box in the CsatFT3 promoter, repressing its expression under low
716 temperatures. Silencing of SVP2 alleviated low-temperature-induced flowering
717 suppression and restored *CsatFT3* expression, thereby establishing a direct
718 mechanistic link between ambient temperature perception and floral induction (Figure
719 5). In *Arabidopsis thaliana*, a comparable regulatory pathway has been described,
720 where SVP negatively regulates FT expression by directly binding to a CArG motif in
721 its promoter (Lee et al., 2007). Additionally, SVP levels are known to increase under
722 low temperatures and are degraded at higher temperatures, facilitating early flowering
723 as SVP abundance declines (Blázquez et al., 2002; Lee et al., 2013a; Sureshkumar
724 et al., 2016). Interestingly, individual members of the SVP gene family have been
725 shown to play distinct roles in processes such as bud dormancy, flowering initiation,
726 and floral development reflecting adaptations of developmental timing to local
727 environmental conditions and seasonal temperature fluctuations. In tulips, gene
728 expression analyses have similarly identified *TgMADS15*/*16* and *TgMADS9* as low-
729 temperature-responsive SVP-like genes involved in floral induction (Lu et al., 2023),
730 reinforcing the conserved role of this gene family in temperature-mediated flowering
731 regulation across geophytic species. SVP homologs in Lilium and *Narcissus tazetta*
732 have also been reported as flowering repressors, though their temperature
733 responsiveness remains unexplored (Li et al., 2015; Wu et al., 2024). Notably, ectopic
734 expression of *CsatSVP2* in Arabidopsis caused floral morphology defects, reminiscent
735 of phenotypes observed with Lilium SVP expression (Wu et al., 2024), suggesting that
736 these homologs may also contribute to flower development in addition to regulating
737 flowering time.
738

739 **Conclusion**

740 Collectively, our findings establish a detailed molecular framework for temperature-
741 regulated flowering in saffron, centered on the dynamic balance between floral
742 activators (CsatFT3, CsatFD2) and repressors (CsatTFL1-3, CsatSVP2). The
743 spatiotemporal expression patterns and protein interactions among these components
744 provide key insights into how flowering is precisely modulated in response to
745 environmental temperature fluctuations. By uncovering saffron-specific adaptations
746 within otherwise conserved gene networks, this study advances our understanding of

747 floral regulation in geophytes and sterile crops. Importantly, these results lay a
748 foundation for the development of genetic and biotechnological strategies to improve
749 saffron yield, synchronize flowering, and enhance resilience to climate variability. Our
750 work highlights a saffron-specific model of thermoresponsive flowering that builds
751 upon conserved floral regulatory pathways, yet exhibits functional divergence shaped
752 by the geophytic lifecycle. Beyond saffron, these findings offer a valuable framework
753 for translational research in other temperature-sensitive geophytes such as tulip,
754 Narcissus, Hyacinthus, and Iris, where molecular insights remain scarce (Khodorova
755 and Boitel-Conti, 2013). By identifying novel regulatory targets, this study opens new
756 avenues for improving flowering and productivity in saffron and related high-value
757 geophytic species.
758

759 **Acknowledgments**

760 We gratefully acknowledge the financial support from the Council of Scientific and
761 Industrial Research (CSIR) under the Genome Editing Mission for Crop Improvement
762 (MMP25301), the intramural CSIR grant to IHBT (MLP201), the SERB-Start-up
763 Research Grant (SRG/GAP0288), and the Department of Biotechnology
764 (DBT/GAP0307) to Rajesh Kumar Singh. Senior Research Fellowships provided to
765 Diksha Kalia (UGC), Joel Jose-Santhi (CSIR), and Firdous Rasool Sheikh (CSIR) are
766 also gratefully acknowledged. We sincerely thank Dr. Rishikesh Bhalerao, Umeå Plant
767 Science Centre, Swedish University of Agricultural Sciences, Sweden, for his careful
768 reading of the manuscript and for providing constructive feedback, which significantly
769 improved the clarity and quality of the work. Our sincere thanks go to Dr. Rimpy Diman,
770 Technical Officer at CSIR-IHBT, for her valuable assistance with confocal microscopy.
771 This manuscript represents the CSIR-IHBT communication number "5819".
772

773 **Author contribution statement**

774 R.K.S. conceptualized the research idea and designed the work plan. D.K., J.J.S., and
775 F.R.S. conducted the experiments and collected the data. D.K., J.J.S., and R.K.S.
776 analyzed the data and contributed to writing the manuscript. All authors read and
777 approved the final version of the manuscript.
778

779 **Conflicts of Interest**

780 The authors declare no conflicts of interest.

781

782 **Figure Legends**

783 **Figure 1. *CsatFT3* is involved in temperature mediated floral induction in saffron.**
784 **(A)** CsatFT3 transcript levels in apical buds across developmental stages show
785 specific expression during the reproductive phase. **(B)** Relative expression of CsatFT3
786 in apical buds of saffron corms stored at ambient (25°C) and low (8°C) temperatures.
787 Data are means ± SEM from 3 biological replications, where n=10 for each replicate.
788 **(C)** Histochemical GUS assay of the *CsatFT3* promoter (proCsatFT3) in transgenic
789 Arabidopsis in long-day conditions (LD) during various developmental stages. 1.2kb
790 sequence upstream of the CsatFT3 translation start sites (proCsatFT3) was fused with
791 uidA (GUS) reporter gene. Different developmental stages include Arabidopsis plants
792 after 7 Days After Germination (DAG), 14DAG, 21DAG, and 30DAG. FT3 expression
793 is confined to meristem and inflorescence **(D)** Temperature sensitive GUS activity at
794 3 different temperatures. The experiment was repeated three times independently with
795 similar results. **(E-G)** Ectopic expression of CsatFT3 in Arabidopsis resulted in early
796 flowering phenotype. Statistical significance was analyzed by Student's t-test (*P <
797 0.05). **(H-J)** Functional complementation of the *ft-1* mutant with CsatFT3 restores
798 flowering. Representative line expressing number of rosette leaves and number of
799 days to flower. Total leaf number was calculated by combining total rosette leaves.
800 Data represent a minimum of 10 plants scored for each line. Statistical significance
801 was analyzed by Student's t-test (*P < 0.05). **(K)** Representative flowering vs. non-
802 flowering phenotypes in control and CsatFT3-silenced saffron corms. The scale bar
803 represents 2 cm. **(L)** qRT-PCR validation of CsatFT3 transcript knockdown in saffron
804 corm apices following VIGS (n=3 technical replicates, 10 independent corms). Error
805 bars are shown as Standard Error of Mean (SEM) of three technical repeats. **(M)**
806 Percentage of flowering in VIGS-silenced vs. TRV2 control corms. The data presented
807 includes the mean percentage of flowering, with error bars representing the Standard
808 Error of Mean (SEM) of three technical repeats (n=3) and for each replicate, 10 corms
809 were used. All data in this figure are shown as mean ± SEM. Statistical Significance
810 for Data in panel A, I, & J are analyzed using one-way ANOVA followed by Tukey's
811 Honest Significant Difference (HSD) test for multiple comparisons. Different letters
812 indicate statistically significant differences between groups at $p < 0.05$, according to
813 Compact Letter Display (CLD). Data in panels B are analyzed using two-way ANOVA
814 to assess the effects of temperature, month, and their interaction, followed by Sidak's

815 multiple comparisons test. Asterisks indicate significant differences between 8°C and
816 25°C within each month (**** $p < 0.0001$), F, **G**, **L**, and **M** are analyzed using the
817 student's t-test (*: $p<0.05$; **: $p<0.01$).
818
819 **Figure 2: Functional characterization of FD-like genes in saffron (A)** Expression
820 profiles of CsatFD1, CsatFD2, and CsatFD3 during vegetative and floral induction
821 stages in the apical bud by RT-qPCR. Data are means ± SE of 3 independent
822 replicates. **(B)** Expression patterns of CsatFD1, CsatFD2, and CsatFD3 in the Main
823 bud (MB), axillary bud (AB), and corm tissue (CT) during the floral induction stage.
824 Values are means ± SE of 3 independent replicates. **(C)** Tissue specific expression of
825 FDs in different parts of saffron plant. **(D)** Expression analyses of *CsatFD* genes in
826 apical buds of corms stored at 25◦ C and 8 during months of May and June (**E)**
827 Phenotypic comparison of early flowering in CsatFD2-expressing Arabidopsis
828 compared to control. **(F-K)** Measurements of days to flowering and rosette leaf number
829 in CsatFD1, CsatFD2, and CsatFD3 expressing Arabidopsis plants. Values are means
830 ± SE (n = 10). Asterisks indicate a significant difference between the transgenic
831 Arabidopsis lines and wild-type plants (Col-0; Student's t-test, $P < 0.05$). **(L)**
832 Phenotypes of CsatFD2-TRV2 silenced lines and TRV2 lines. The scale bar
833 represents 2 cm. **(M)** qRT-PCR validation of CsatFD2 knockdown in saffron corm
834 apices after VIGS (n=3). Error bars are shown as SD of three technical repeats **(N)**
835 Flowering percentage in TRV2 control and CsatFD2 VIGS-silenced saffron corms. The
836 data presented includes the mean percentage of flowering, with error bars
837 representing the standard error of mean (SEM) of three technical repeats (n=3) and
838 for each replicate, 10 corms were used. All data in this figure are shown as mean ±
839 SEM. Statistical Significance for data in panel **A** & **B** are analyzed using two-way
840 ANOVA followed by Tukey's Honest Significant Difference (HSD) test for multiple
841 comparisons. Different letters indicate statistically significant differences between
842 groups at $p < 0.05$, according to Compact Letter Display (CLD). Data in panel **D** are
843 analyzed using two-way ANOVA to assess the effects of temperature, month, and their
844 interaction, followed by Sidak's multiple comparisons test. Asterisks indicate
845 significant differences between 8°C and 25°C within each month (**** $p < 0.0001$),
846 **F**,**G**,**H**,**I**,**J**,**K**,**M** and **N** are analyzed using the Student's t-test (*: $p<0.05$; **: $p<0.01$).
847

848 **Figure 3: CsatTFL1-3 is negative regulator of floral induction in saffron (A)**
849 Relative expression of CsatTFL1-3 during vegetative and reproductive phase in the
850 apical bud by RT-qPCR. Data are means ± SE of 3 independent replicates. **(B)**
851 Expression analyses of CsatTFL1-3 gene in apical buds of corms stored at 25°C and
852 8 °C during floral induction time **(C)** Corm tissue specific expression of TFL1-3 during
853 floral induction. **(D)** Tissue Specific Expression of CsatTFL1-3. **(E)**Phenotypic analysis
854 of Arabidopsis Col-0 plants ectopically expressing TFL1-3/CEN1, Hyper vegetive
855 phase phenotype observed in CsatTFL1-3 transgenic lines of Arabidopsis. **(F and G)**
856 Rosette leaves number and number of days to flower of 35S::TFL1-3 transgenic and
857 control plants respectively. Values are means ± SEM (n = 10). Asterisks indicate a
858 significant difference between the transgenic Arabidopsis lines and wild-type plants
859 (Col-0; Student's t-test, P < 0.05). **(H)** Virus-Induced Gene Silencing (VIGS) of TFL1-
860 3/CEN1 in low-flower-competent saffron corms. The scale bar represents 2 cm. **(I)** The
861 expression of *CsatTFL1-3* in *CsatTFL1-3*-TRV2 silenced lines and TRV2 lines (n=3).
862 **(J)** Comparison of flowering percentages in VIGS-silenced versus control saffron
863 corms. The data presented includes the mean percentage of flowering of three
864 technical repeats (n=3) and for each replicate, 10 corms were used. All data in this
865 figure are shown as mean ± SEM. Statistical Significance for Data in panel **A**, **C** & **D**
866 are analyzed using one-way ANOVA followed by Tukey's Honest Significant
867 Difference (HSD) test for multiple comparisons. Different letters indicate statistically
868 significant differences between groups at p < 0.05, according to Compact Letter
869 Display (CLD). Data in panel B are analyzed using two-way ANOVA to assess the
870 effects of temperature, month, and their interaction, followed by Sidak's multiple
871 comparisons test. Asterisks indicate significant differences between 8°C and 25°C
872 within each month (**** p < 0.0001), F,G,I, & J are analyzed using the Student's t-test
873 (*: p<0.05; **: p<0.01).
874
875 **Figure 4. Interaction analysis of CsatFT3, CsatTFL1-3, and CsatFD2.**
876 **(A, B)** Yeast two-hybrid (Y2H) assays showing physical interactions between
877 CsatFT3/CsatTFL1-3 and CsatFD2. The coding sequences of *CsatFT3* and
878 *CsatTFL1-3* were fused to the activation domain in the pGADT7 vector, and *CsatFD2*
879 was fused to the DNA-binding domain in the pGBKT7 vector. Yeast transformants
880 were grown on double dropout (DDO) medium lacking tryptophan and leucine
881 (selection for transformation) and quadruple dropout (QDO) medium lacking

882 tryptophan, leucine, histidine, and adenine (selection for interaction). pGBKT7-53 and
883 pGADT7-T were used as positive control; pGBKT7-lam and pGADT7-T interactions
884 served as the negative control. **(C-D)** Bimolecular fluorescence complementation
885 (BiFC) assay showing nuclear localization of the interactions between CsatFT3 or
886 CsatTFL1-3 with CsatFD2 in *Nicotiana benthamiana* leaf epidermal cells. CsatFD2
887 was fused to the C-terminal half of YFP (cYFP), and CsatFT3 or CsatTFL1-3 were
888 fused to the N-terminal half of YFP (nYFP). YFP signal indicates interaction. Bars =
889 20 μm. **(E)** Competitive luciferase complementation assay demonstrating the
890 competition between CsatFT3 and CsatTFL1-3 for binding to CsatFD2 in *N.*
891 *benthamiana* leaves. CsatTFL1 was fused to the N-terminal half of luciferase (nLUC),
892 and CsatFD2 to the C-terminal half (cLUC). Increasing amounts of CsatFT3 (non-
893 tagged, driven by 35S promoter, in SK vector) were co-infiltrated at different ratios.
894 Images represents three independent replications. **(F)** Relative luminescence
895 intensities indicate competition for FD2 binding with TFL1-3 and FT3. Data
896 represented is mean of three replicates. Statistical Significance are analyzed using
897 one-way ANOVA followed by Tukey's Honest Significant Difference (HSD) test for
898 multiple comparisons. Different letters indicate statistically significant differences
899 between groups at $p < 0.05$, according to Compact Letter Display (CLD).
900
901 **Figure 5: Functional characterization of CsatSVP1 and CsatSVP2 in**
902 **temperature-dependent floral regulation (A)** Expression profiling of CsatSVP1 and
903 CsatSVP2 in apical bud during different vegetative and flowering stages. Data are
904 means ± SE from 3 replications. **(B and C)** Expression of SVP1 and SVP2 genes in
905 corms stored at inductive (25°C) and non-inductive (8°C) temperatures respectively.
906 **(D)** Flowering phenotypes of Arabidopsis lines ectopically expressing CsatSVP1. **(E**
907 **and F)** Rosette leaves number and number of days to flower of CsatSVP1 transgenic
908 and control plants respectively **(G)** Phenotypic changes of the floral organs in
909 35S::CsatSVP2 transgenic Arabidopsis plants. **(H-I)** Rosette leaves number and
910 number of days to flower of CsatSVP2 transgenic and control plants respectively. The
911 total leaf number was calculated by combining total rosette leaves. **(J-K)** Silencing of
912 CsatSVP2 by VIGS rescues flowering under low-temperature conditions in saffron.
913 The scale bar represents 2 cm. **(L-M)** qRT-PCR validation of CsatSVP2 knockdown in
914 saffron corm apices after VIGS stored at different temperatures (n=3). Error bars are
915 shown as SD of three technical repeats. **(N-O)** Flowering percentage in TRV2 control

916 and CsatSVP2 VIGS-silenced saffron corms stored at low (8°C) and ambient (23°C)
917 temperatures. The data presented includes the mean percentage of flowering, with
918 error bars representing the standard deviation (SD) of three technical repeats (n=3)
919 and for each replicate, 10 corms were used. **(P-Q)** Relative expression of CsatFT3 in
920 SVP2-silenced versus control corms under different temperature regimes. All data in
921 this figure are shown as mean ± SEM. Statistical Significance for data in panel A are
922 analyzed using two-way ANOVA followed by Tukey's Honest Significant Difference
923 (HSD) test for multiple comparisons. Different letters indicate statistically significant
924 differences between groups at $p < 0.05$, according to Compact Letter Display (CLD).
925 Data in panel B & C are analyzed using two-way ANOVA to assess the effects of
926 temperature, month, and their interaction, followed by Sidak's multiple comparisons
927 test. Asterisks indicate significant differences between 8°C and 25°C within each
928 month (**** $p < 0.0001$), E, F, H, I, L, M, N, O, P & Q are analyzed using the student's
929 t-test (*: $p<0.05$; **: $p<0.01$).
930
931 **Figure 6. CsatSVP2 directly binds to the FT3 promoter via the CArG motif and**
932 **represses its transcription (A)** Schematic diagram of the 1.2 kb CsatFT3 promoter
933 showing the location of a conserved CArG-box motif (CCATTTAAGG) approximately
934 827 bp upstream of the ATG start codon. **(B)** Yeast one-hybrid assay showing
935 interaction between CsatSVP2 and the FT3 promoter region containing the CArG
936 motif. Growth on selective media confirms binding specificity. **(C)** Schematic diagram
937 of the effectors and reporters used in dual-luciferase reporter. **(D)** Schematic of the
938 dual-luciferase constructs used for transient expression in *Nicotiana benthamiana*: FL
939 (Full length promoter) T1 (with CArG motif) and T2 (without). **(E)** Relative luciferase
940 activity in leaves co-expressing CsatSVP2 with the full promoter and T1 fragment
941 construct of *CsatFT3* gene. **(F)** Relative luciferase activity in leaves co-expressing
942 CsatSVP2 and CsatFT3 full promoter and with T2 fragment constructs. Significant
943 repression is observed only in the T1 construct, indicating that CsatSVP2 represses
944 *CsarFT3* transcription through the CArG motif. **(G and H)** Quantification of luciferase
945 activity. Bars represent mean ± SEM (n = 3). All data in figure are shown as mean ±
946 SEM. Statistical Significance for Data in panel **F** & **H** areanalyzed using one-way
947 ANOVA followed by Tukey's Honest Significant Difference (HSD) test for multiple
948 comparisons. Different letters indicate statistically significant differences between
949 groups at $p < 0.05$, according to Compact Letter Display (CLD)

**Figure 7. Proposed model of temperature-mediated flowering regulation in saffron.** This schematic model illustrates the temperature-regulated floral induction pathway in saffron, emphasizing the key roles of CsatFT3, CsatFD2, TFL1-3/CEN1, and CsatSVP2 in transitioning from vegetative to reproductive growth. At low temperatures (e.g., below 10°C), *CsatFT3* expression remains low, and TFL1-3/CEN1 binds to CsatFD2, preventing the formation of the Floral Activator Complex (FAC) and maintaining the shoot apical meristem in a vegetative state and inhibiting flowering. Additionally, CsatSVP2 is upregulated at low temperatures and binds directly to a conserved CArG motif in the CsatFT3 promoter, repressing its transcription and reinforcing the suppression of flowering. As temperatures increase beyond a critical threshold (e.g., above 25 °C), CsatFT3 expression is upregulated, enabling its interaction with CsatFD2 to form the FAC, which in turn activates floral meristem identity genes and promotes floral initiation. Concurrently, TFL1-3/CEN1 expression is downregulated, releasing the repression on CsatFD2 and facilitating the transition to reproductive development.

984 **Figure 1**

985

986

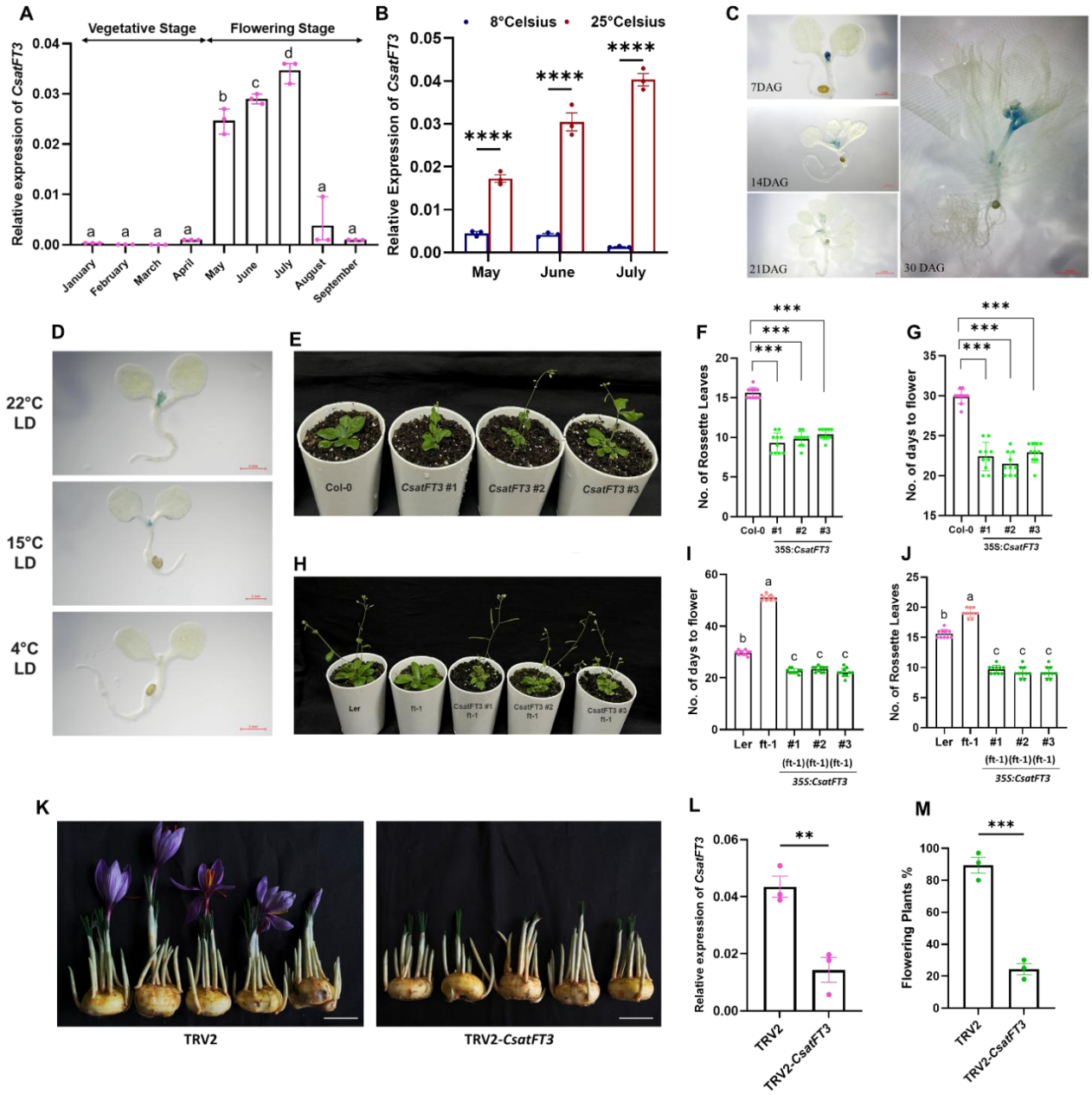


987

988

989

990

991

992

993

994 **Figure 2**

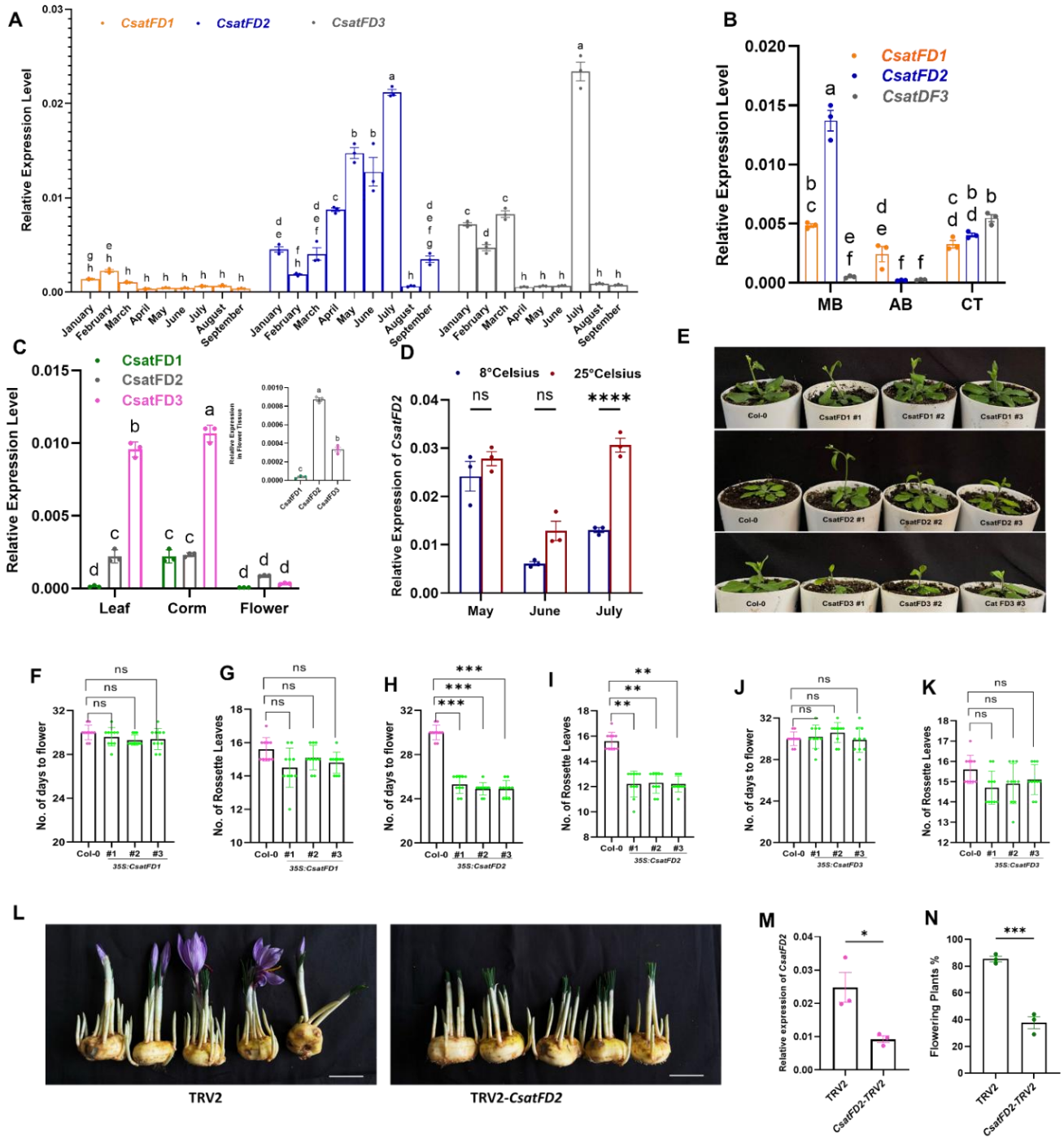


995

996

997

998

999

1000

1001 **Figure 3**

1002

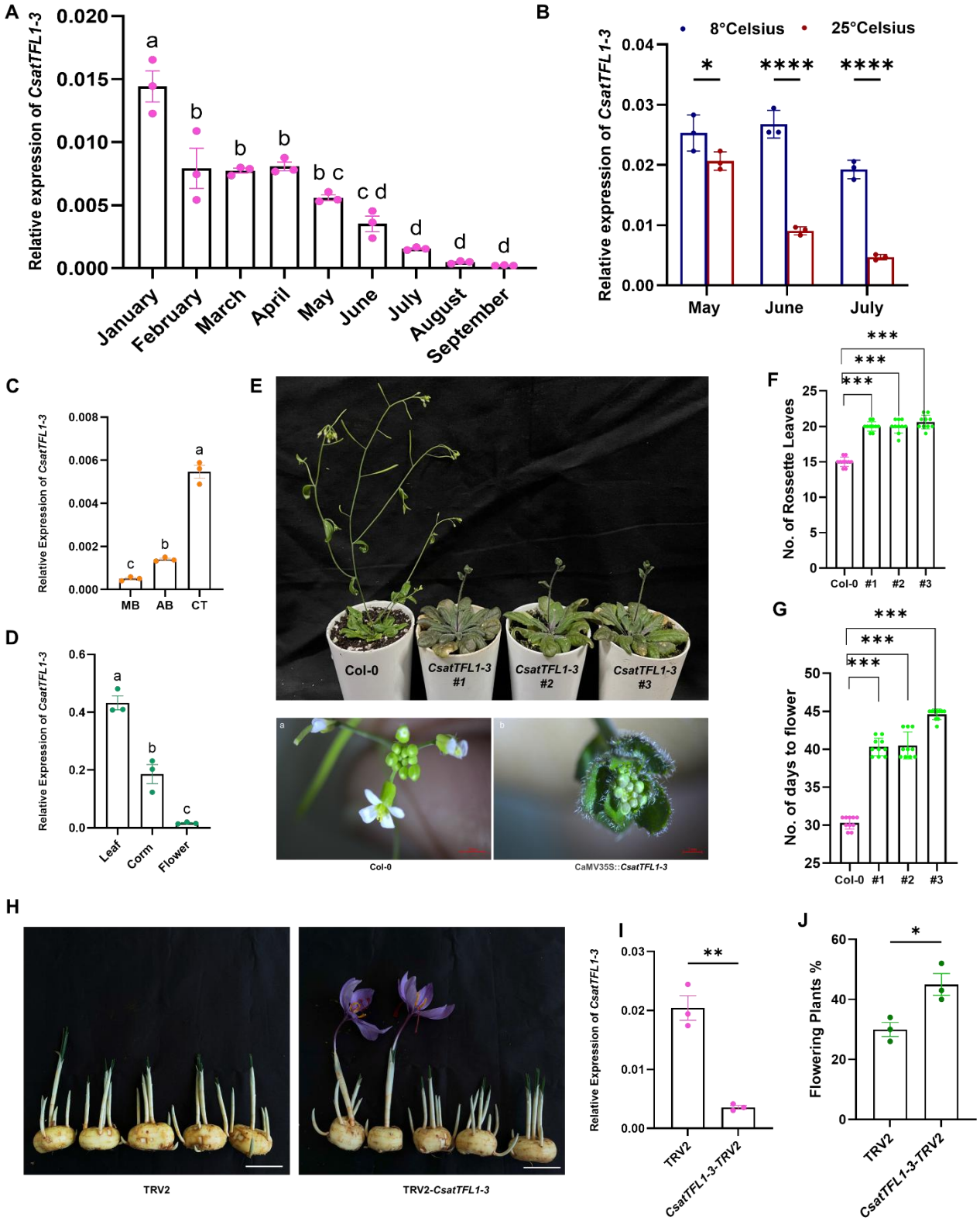


1003

1004

1005 **Figure 4**

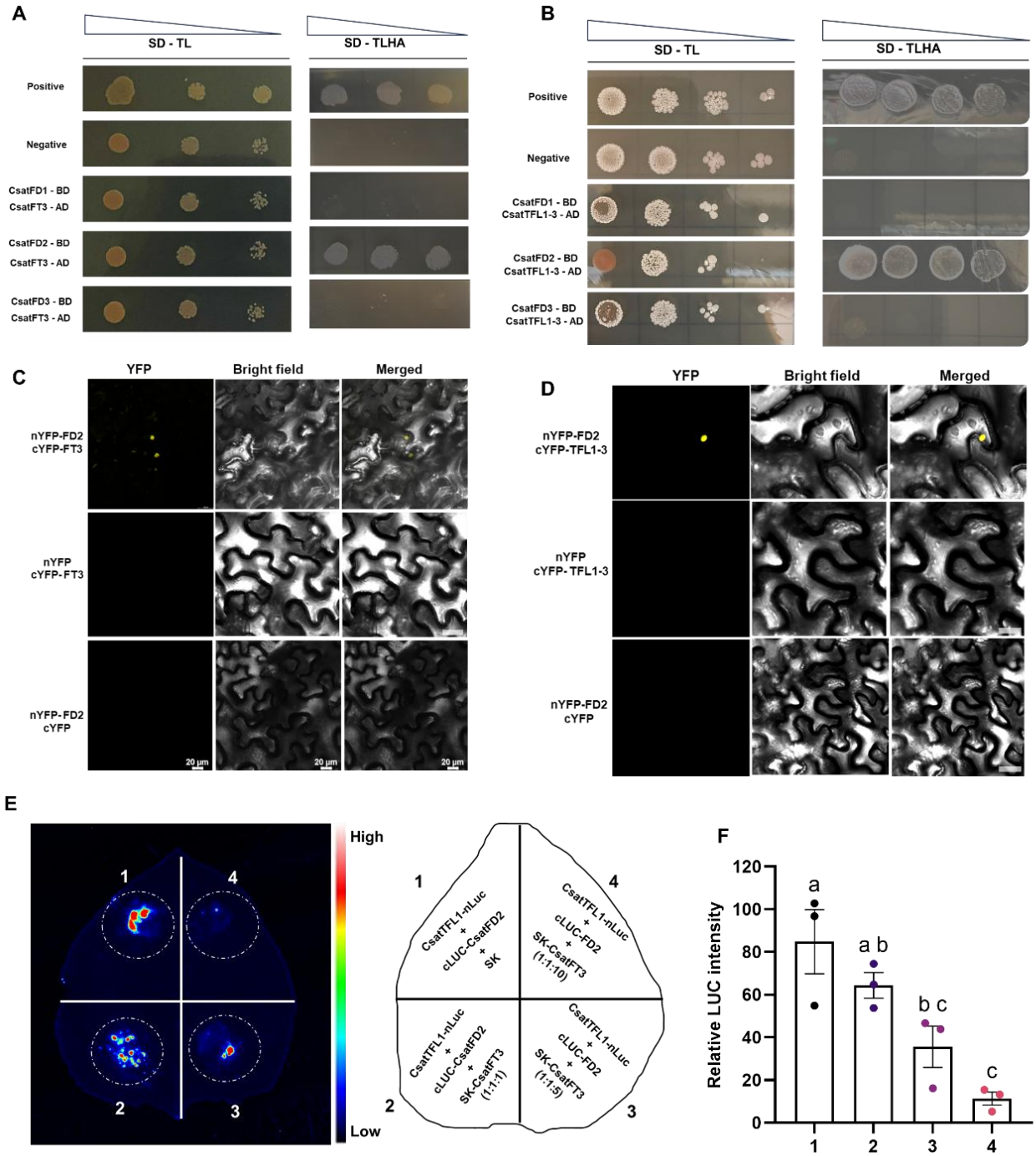


1006

1007

1008

1009

1010

1011

1012

1013 **Figure 5**

1014

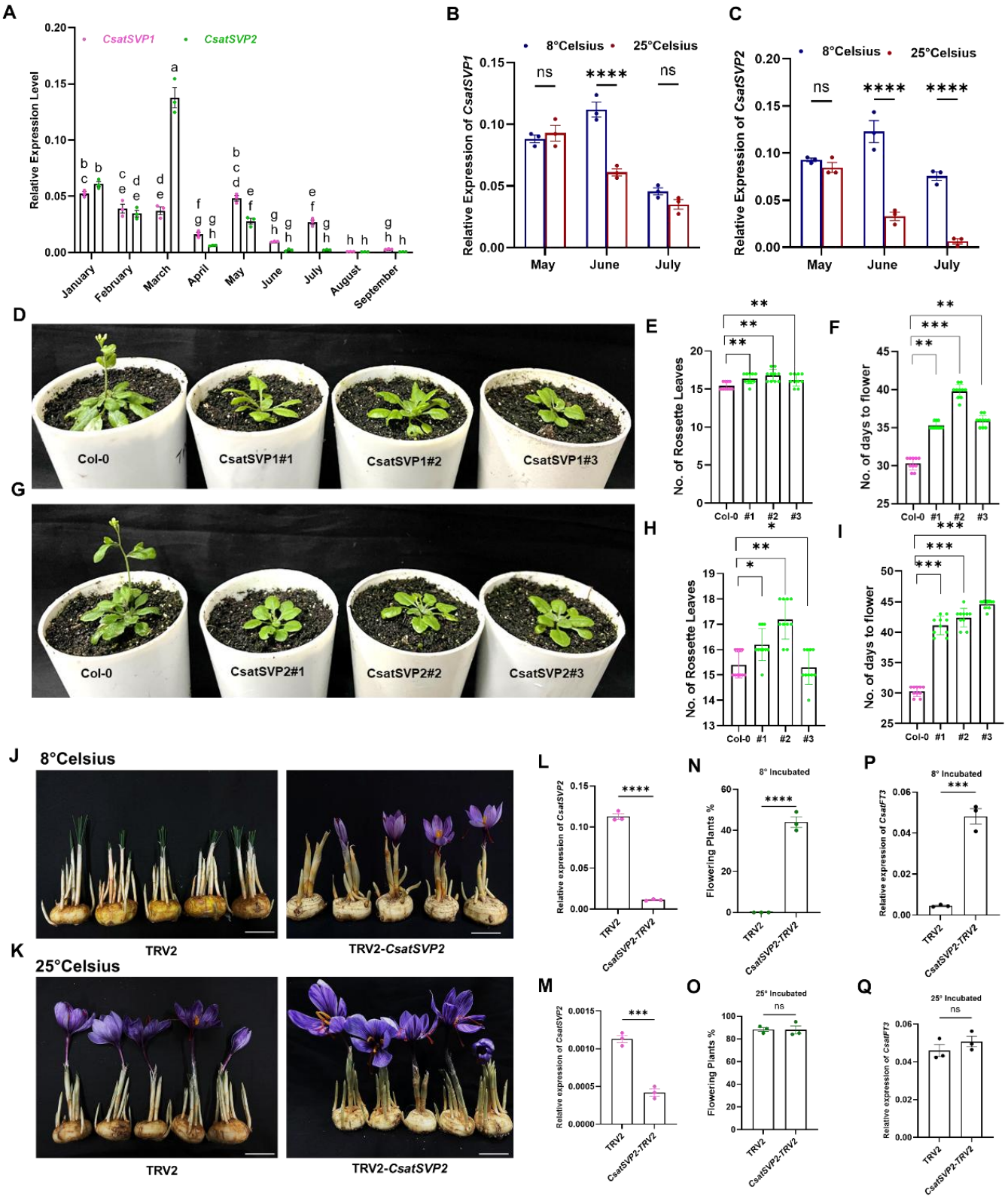


1015

1016

1017

1018

1019 **Figure 6**

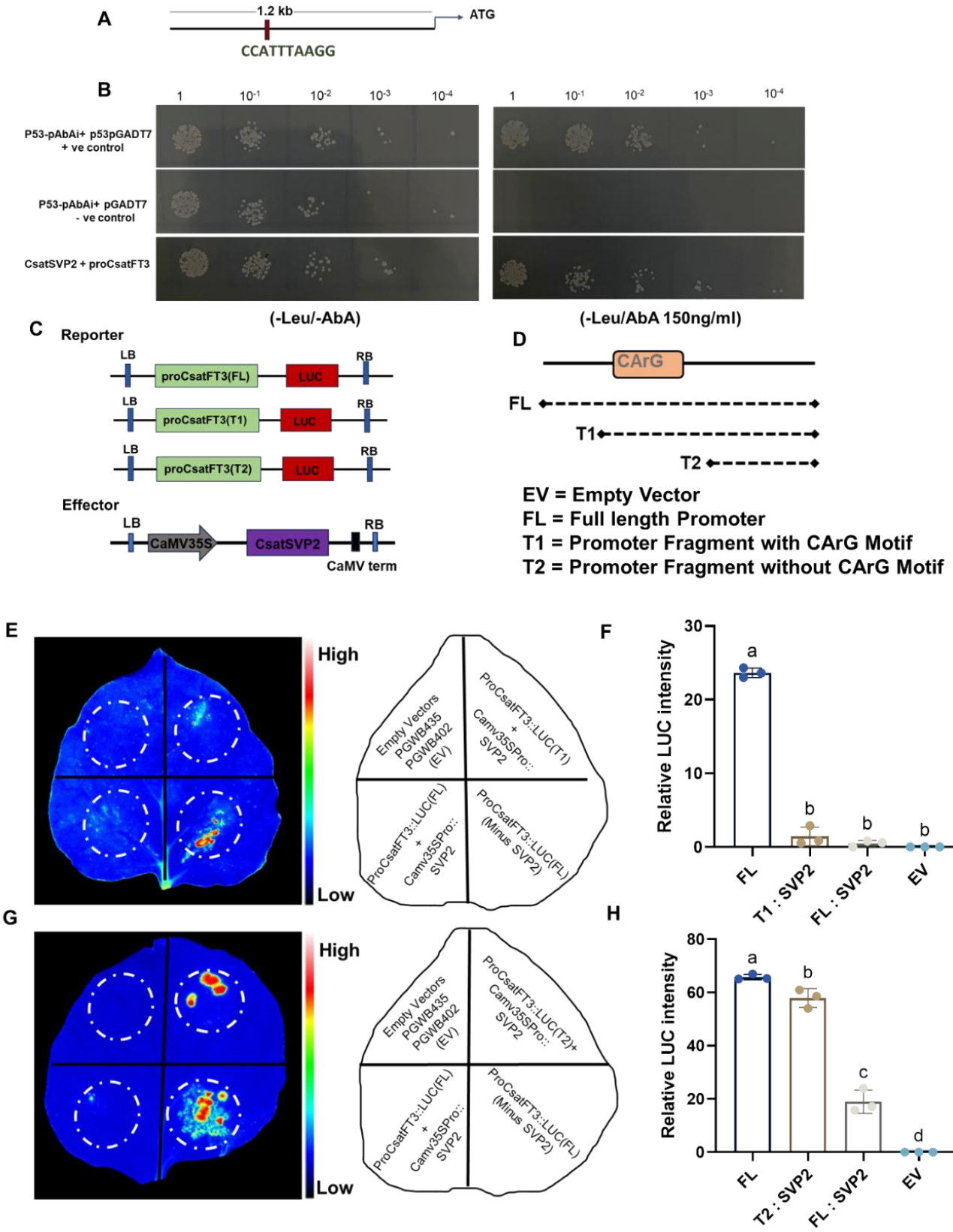


1020

1021 **Figure 7**

1022

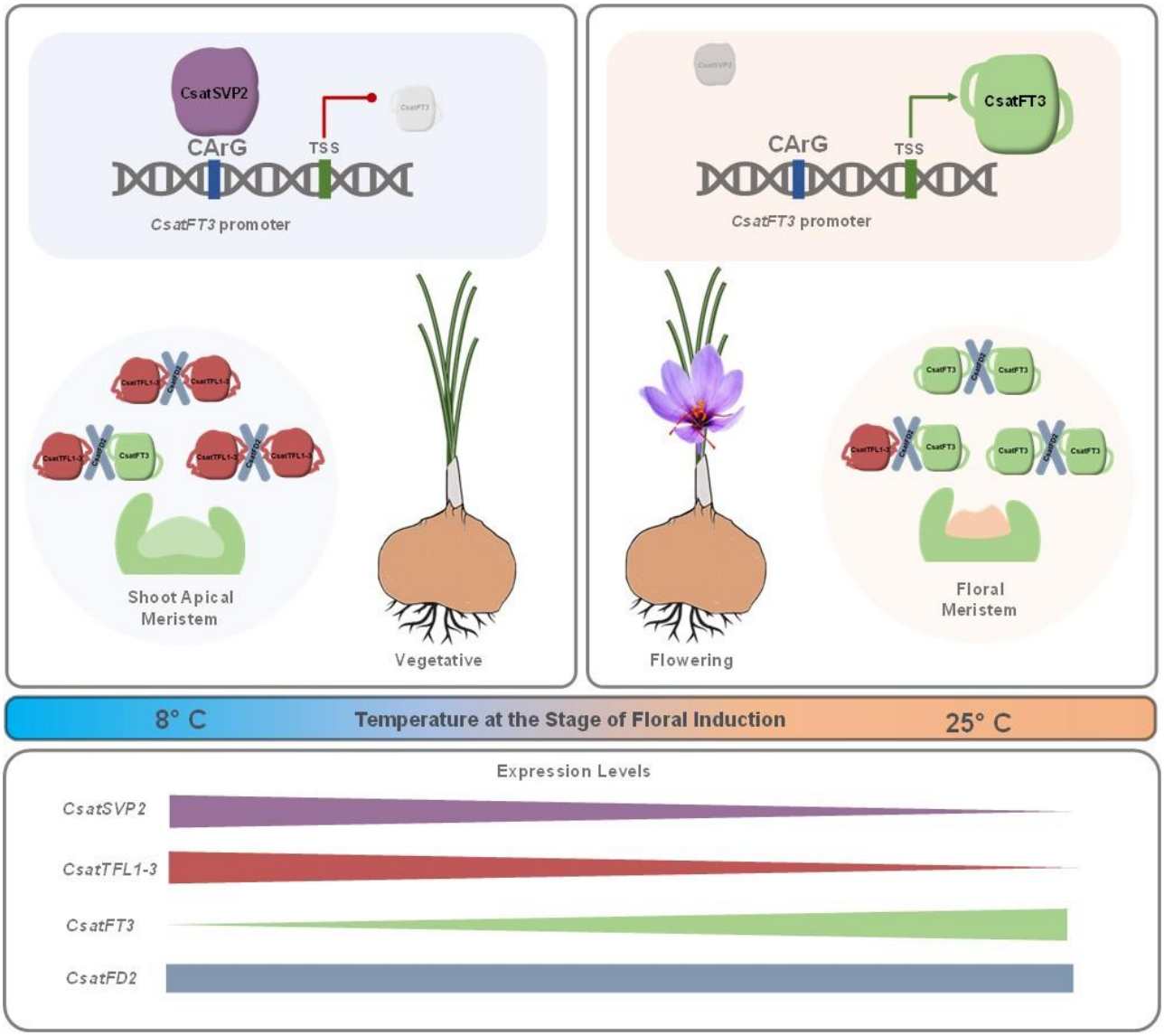


1023

1024

1025

1026

1027

1028

1029

1030

1031

1032

1033

1034

1035 ## References


1036 Abe, M., Kobayashi, Y., Yamamoto, S., Daimon, Y., Yamaguchi, A., Ikeda, Y., Ichinoki, H., Notaguchi, M.,
1037 Goto, K. and Araki, T. (2005) FD, a bZIP protein mediating signals from the floral pathway
1038 integrator FT at the shoot apex. *Science* **309**, 1052-1056.
1039 Ahrazem, O., Rubio-Moraga, A., Nebauer, S.G., Molina, R.V. and Gomez-Gomez, L. (2015) Saffron: Its
1040 Phytochemistry, Developmental Processes, and Biotechnological Prospects. *J Agric Food Chem*
1041 **63**, 8751-8764.
1042 Andrés, F. and Coupland, G. (2012) The genetic basis of flowering responses to seasonal cues. *Nature*
1043 *Reviews Genetics* **13**, 627-639.
1044 Balasubramanian, S., Sureshkumar, S., Lempe, J. and Weigel, D. (2006) Potent induction of Arabidopsis
1045 thaliana flowering by elevated growth temperature. *PLoS genetics* **2**, e106.
1046 Bellinazzo, F., Manders, I., Heidemann, B., Bolanos, M.A., Stouten, E., Busscher, J., Abarca, D., van der
1047 Wal, F., Dornelas, M.C. and Angenent, G.C. (2025) Differential growth and flowering capacity
1048 of tulip bulbs and the potential involvement of PHOSPHATIDYLETHANOLAMINE-BINDING
1049 PROTEINS (PEBPs). *Biology Direct* **20**, 29.
1050 Blázquez, M.A., Trénor, M. and Weigel, D. (2002) Independent control of gibberellin biosynthesis and
1051 flowering time by the circadian clock in Arabidopsis. *Plant Physiology* **130**, 1770-1775.
1052 Bowman, J.L., Smyth, D.R. and Meyerowitz, E.M. (2012) The ABC model of flower development: then
1053 and now. *Development* **139**, 4095-4098.
1054 Capovilla, G., Schmid, M. and Posé, D. (2015) Control of flowering by ambient temperature. *Journal of*
1055 *Experimental Botany* **66**, 59-69.
1056 Cardone, L., Castronuovo, D., Perniola, M., Cicco, N. and Candido, V. (2020) Saffron (Crocus sativus L.),
1057 the king of spices: An overview. *Scientia Horticulturae* **272**, 109560.
1058 Freytes, S.N., Canelo, M. and Cerdán, P.D. (2021) Regulation of flowering time: when and where?
1059 *Current Opinion in Plant Biology* **63**, 102049.
1060 Gu, X., Le, C., Wang, Y., Li, Z., Jiang, D., Wang, Y. and He, Y. (2013) Arabidopsis FLC clade members
1061 form flowering-repressor complexes coordinating responses to endogenous and
1062 environmental cues. *Nature Communications* **4**, 1947.
1063 Heide, O.M. (1977) Photoperiod and temperature interactions in growth and flowering of strawberry.
1064 *Physiologia Plantarum* **40**, 21-26.
1065 Hsu, C.-Y., Adams, J.P., Kim, H., No, K., Ma, C., Strauss, S.H., Drnevich, J., Vandervelde, L., Ellis, J.D. and
1066 Rice, B.M. (2011) FLOWERING LOCUS T duplication coordinates reproductive and vegetative
1067 growth in perennial poplar. *Proceedings of the National Academy of Sciences* **108**, 10756-
1068 10761.
1069 Hu, J., Liu, Y., Tang, X., Rao, H., Ren, C., Chen, J., Wu, Q., Jiang, Y., Geng, F. and Pei, J. (2020)
1070 Transcriptome profiling of the flowering transition in saffron (Crocus sativus L.). *Scientific*
1071 *Reports* **10**, 9680.
1072 Jefferson, R.A., Kavanagh, T.A. and Bevan, M.W. (1987) GUS fusions: beta-glucuronidase as a sensitive
1073 and versatile gene fusion marker in higher plants. *Embo j* **6**, 3901-3907.
1074 Jin, S. and Ahn, J.H. (2021) Regulation of flowering time by ambient temperature: repressing the
1075 repressors and activating the activators. *New Phytologist* **230**, 938-942.
1076 Jin, S., Nasim, Z., Susila, H. and Ahn, J.H. (2021) Evolution and functional diversification of FLOWERING
1077 LOCUS T/TERMINAL FLOWER 1 family genes in plants. *Seminars in Cell & Developmental*
1078 *Biology* **109**, 20-30.
1079 Jing, S., Jiang, P., Sun, X., Yu, L., Wang, E., Qin, J., Zhang, F., Prat, S. and Song, B. (2023) Long-distance
1080 control of potato storage organ formation by SELF PRUNING 3D and FLOWERING LOCUS T-like
1081 1. *Plant communications* **4**.

1082 Jose-Santhi, J., Sheikh, F.R., Kalia, D. and Singh, R.K. (2023) Sugar metabolism mediates temperature-
1083 dependent flowering induction in saffron (Crocus sativus L.). *Environmental and Experimental*
1084 *Botany* **206**, 105150.
1085 Kalia, D., Jose-Santhi, J., Kumar, R. and Singh, R.K. (2022) Analysis of PEBP Genes in Saffron Identifies
1086 a Flowering Locus T Homologue Involved in Flowering Regulation. *Journal of Plant Growth*
1087 *Regulation*, 1-20.
1088 Kalia, D., Jose-Santhi, J., Kumar, R. and Singh, R.K. (2023) Analysis of PEBP genes in saffron identifies a
1089 flowering locus T homologue involved in flowering regulation. *Journal of Plant Growth*
1090 *Regulation* **42**, 2486-2505.
1091 Kalia, D., Jose-Santhi, J., Sheikh, F.R., Singh, D. and Singh, R.K. (2024) Tobacco rattle virus-based virus-
1092 induced gene silencing (VIGS) as an aid for functional genomics in Saffron (Crocus sativus L.).
1093 *Physiol Mol Biol Plants* **30**, 749-755.
1094 Khodorova, N.V. and Boitel-Conti, M. (2013) The role of temperature in the growth and flowering of
1095 geophytes. *Plants* **2**, 699-711.
1096 Khosa, J., Bellinazzo, F., Kamenetsky Goldstein, R., Macknight, R. and Immink, R.G.H. (2021)
1097 PHOSPHATIDYLETHANOLAMINE-BINDING PROTEINS: the conductors of dual reproduction in
1098 plants with vegetative storage organs. *Journal of Experimental Botany* **72**, 2845-2856.
1099 Kinoshita, A. and Richter, R. (2020) Genetic and molecular basis of floral induction in Arabidopsis
1100 thaliana. *Journal of Experimental Botany* **71**, 2490-2504.
1101 Komiya, R., Ikegami, A., Tamaki, S., Yokoi, S. and Shimamoto, K. (2008) Hd3a and RFT1 are essential
1102 for flowering in rice.
1103 Lee, C., Kim, S.J., Jin, S., Susila, H., Youn, G., Nasim, Z., Alavilli, H., Chung, K.S., Yoo, S.J. and Ahn, J.H.
1104 (2019) Genetic interactions reveal the antagonistic roles of FT/TSF and TFL1 in the
1105 determination of inflorescence meristem identity in Arabidopsis. *The Plant Journal* **99**, 452-
1106 464.
1107 Lee, J.H., Ryu, H.-S., Chung, K.S., Posé, D., Kim, S., Schmid, M. and Ahn, J.H. (2013a) Regulation of
1108 Temperature-Responsive Flowering by MADS-Box Transcription Factor Repressors. *Science*
1109 **342**, 628-632.
1110 Lee, J.H., Yoo, S.J., Park, S.H., Hwang, I., Lee, J.S. and Ahn, J.H. (2007) Role of SVP in the control of
1111 flowering time by ambient temperature in Arabidopsis. *Genes & development* **21**, 397-402.
1112 Lee, R., Baldwin, S., Kenel, F., McCallum, J. and Macknight, R. (2013b) FLOWERING LOCUS T genes
1113 control onion bulb formation and flowering. *Nat Commun* **4**, 2884.
1114 Leeggangers, H.A., Nijveen, H., Bigas, J.N., Hilhorst, H.W. and Immink, R.G. (2017a) Molecular
1115 Regulation of Temperature-Dependent Floral Induction in Tulipa gesneriana. *Plant Physiol*
1116 **173**, 1904-1919.
1117 Leeggangers, H.A., Nijveen, H., Bigas, J.N., Hilhorst, H.W. and Immink, R.G. (2017b) Molecular
1118 regulation of temperature-dependent floral induction in Tulipa gesneriana. *Plant physiology*
1119 **173**, 1904-1919.
1120 Li, X.-F., Wu, W.-T., Zhang, X.-P., Qiu, Y., Zhang, W., Li, R., Xu, J., Sun, Y., Wang, Y. and Xu, L. (2015)
1121 Narcissus tazetta SVP-like gene NSVP1 affects flower development in Arabidopsis. *Journal of*
1122 *Plant Physiology* **173**, 89-96.
1123 Lu, J., Qu, L., Xing, G., Liu, Z., Lu, X. and Han, X. (2023) Genome-Wide Identification and Expression
1124 Analysis of the MADS Gene Family in Tulips (Tulipa gesneriana). *Genes (Basel)* **14**.
1125 Molina, R., Valero, M., Navarro, Y., Guardiola, J. and Garcia-Luis, A. (2005a) Temperature effects on
1126 flower formation in saffron (Crocus sativus L.). *Scientia horticulturae* **103**, 361-379.
1127 Molina, R.V., M., V., Y., N., A., G.-L. and and Guardiola, J.L. (2005b) Low temperature storage of corms
1128 extends the flowering season of saffron (Crocus sativus L.). *The Journal of Horticultural Science*
1129 *and Biotechnology* **80**, 319-326.
1130 Nakagawa, M., Shimamoto, K. and Kyozuka, J. (2002) Overexpression of RCN1 and RCN2, rice
1131 TERMINAL FLOWER 1/CENTRORADIALIS homologs, confers delay of phase transition and
1132 altered panicle morphology in rice. *The Plant Journal* **29**, 743-750.

1133 Nakano, Y., Higuchi, Y., Sumitomo, K. and Hisamatsu, T. (2013) Flowering retardation by high
1134 temperature in chrysanthemums: involvement of FLOWERING LOCUS T-like 3 gene
1135 repression. *Journal of Experimental Botany* **64**, 909-920.
1136 Navarro, C., Abelenda, J.A., Cruz-Oró, E., Cuéllar, C.A., Tamaki, S., Silva, J., Shimamoto, K. and Prat, S.
1137 (2011) Control of flowering and storage organ formation in potato by FLOWERING LOCUS T.
1138 *Nature* **478**, 119-122.
1139 Noy-Porat, T., Cohen, D., Mathew, D., Eshel, A., Kamenetsky, R. and Flaishman, M.A. (2013) Turned on
1140 by heat: differential expression of FT and LFY-like genes in Narcissus tazetta during floral
1141 transition. *Journal of experimental botany* **64**, 3273-3284.
1142 Oda, A., Narumi, T., Li, T., Kando, T., Higuchi, Y., Sumitomo, K., Fukai, S. and Hisamatsu, T. (2012)
1143 CsFTL3, a chrysanthemum FLOWERING LOCUS T-like gene, is a key regulator of photoperiodic
1144 flowering in chrysanthemums. *Journal of Experimental Botany* **63**, 1461-1477.
1145 Pin, P.A., Benlloch, R., Bonnet, D., Wremerth-Weich, E., Kraft, T., Gielen, J.J. and Nilsson, O. (2010) An
1146 antagonistic pair of FT homologs mediates the control of flowering time in sugar beet. *Science*
1147 **330**, 1397-1400.
1148 Putterill, J., Laurie, R. and Macknight, R. (2004) It's time to flower: the genetic control of flowering
1149 time. *BioEssays* **26**, 363-373.
1150 Pyo, Y., Park, S., Xi, Y. and Sung, S. (2014) Regulation of flowering by vernalisation in Arabidopsis. In:
1151 *Advances in botanical research* pp. 29-61. Elsevier.
1152 Renau-Morata, B., Nebauer, S.G., García-Carpintero, V., Cañizares, J., Gómez Minguet, E., de los
1153 Mozos, M. and Molina, R.V. (2021) Flower induction and development in saffron: Timing and
1154 hormone signalling pathways. *Industrial Crops and Products* **164**, 113370.
1155 Simon, R., Igeño, M.I. and Coupland, G. (1996) Activation of floral meristem identity genes in
1156 Arabidopsis. *Nature* **384**, 59-62.
1157 Singh, D., Sharma, S., Jose-Santhi, J., Kalia, D. and Singh, R.K. (2023) Hormones regulate the flowering
1158 process in saffron differently depending on the developmental stage. *Front Plant Sci* **14**,
1159 1107172.
1160 Srikanth, A. and Schmid, M. (2011) Regulation of flowering time: all roads lead to Rome. *Cellular and*
1161 *molecular life sciences* **68**, 2013-2037.
1162 Strasser, B., Alvarez, M.J., Califano, A. and Cerdán, P.D. (2009) A complementary role for ELF3 and TFL1
1163 in the regulation of flowering time by ambient temperature. *The Plant Journal* **58**, 629-640.
1164 Sureshkumar, S., Dent, C., Seleznev, A., Tasset, C. and Balasubramanian, S. (2016) Nonsense-mediated
1165 mRNA decay modulates FLM-dependent thermosensory flowering response in Arabidopsis.
1166 *Nat Plants* **2**, 16055.
1167 Tamaki, S., Matsuo, S., Wong, H.L., Yokoi, S. and Shimamoto, K. (2007) Hd3a protein is a mobile
1168 flowering signal in rice. *Science* **316**, 1033-1036.
1169 Taoka, K.-i., Ohki, I., Tsuji, H., Kojima, C. and Shimamoto, K. (2013) Structure and function of florigen
1170 and the receptor complex. *Trends in plant science* **18**, 287-294.
1171 Tsaftaris, A., Pasentsis, K. and Argiriou, A. (2013) Cloning and Characterization of FLOWERING LOCUS
1172 T-Like Genes from the Perennial Geophyte Saffron Crocus (Crocus sativus). *Plant Mol. Biol.*
1173 *Report.* **31**, 1558–1568.
1174 Tsuji, H., Nakamura, H., Taoka, K. and Shimamoto, K. (2013) Functional diversification of FD
1175 transcription factors in rice, components of florigen activation complexes. *Plant Cell Physiol*
1176 **54**, 385-397.
1177 Turck, F., Fornara, F. and Coupland, G. (2008) Regulation and identity of florigen: FLOWERING LOCUS
1178 T moves center stage. *Annu. Rev. Plant Biol.* **59**, 573-594.
1179 Tylewicz, S., Tsuji, H., Miskolczi, P., Petterle, A., Azeez, A., Jonsson, K., Shimamoto, K. and Bhalerao,
1180 R.P. (2015) Dual role of tree florigen activation complex component FD in photoperiodic
1181 growth control and adaptive response pathways. *Proceedings of the National Academy of*
1182 *Sciences* **112**, 3140-3145.

1183 Wang, Z., Li, X., Xu, J., Yang, Z. and Zhang, Y. (2021) Effects of ambient temperature on flower initiation
1184 and flowering in saffron (Crocus sativus L.). *Scientia Horticulturae* **279**, 109859.
1185 Wickland, D.P. and Hanzawa, Y. (2015) The FLOWERING LOCUS T/TERMINAL FLOWER 1 gene family:
1186 functional evolution and molecular mechanisms. *Molecular plant* **8**, 983-997.
1187 Wigge, Philip A. (2011) FT, A Mobile Developmental Signal in Plants. *Current Biology* **21**, R374-R378.
1188 Wigge, P.A., Kim, M.C., Jaeger, K.E., Busch, W., Schmid, M., Lohmann, J.U. and Weigel, D. (2005)
1189 Integration of spatial and temporal information during floral induction in Arabidopsis. *Science*
1190 **309**, 1056-1059.
1191 Wu, X., Ling, W., Pan, Y., Yang, Z., Ma, J., Yang, Y., Xiang, W., Zhou, L., Sun, M., Chen, J., Chen, H., Zheng,
1192 S., Zeng, J. and Li, Y. (2024) Functional analysis of a lily SHORT VEGETATIVE PHASE ortholog in
1193 flowering transition and floral development. *Plant Physiology and Biochemistry* **206**, 108287.
1194 Wu, Y.-M., Ma, Y.-J., Wang, M., Zhou, H., Gan, Z.-M., Zeng, R.-F., Ye, L.-X., Zhou, J.-J., Zhang, J.-Z. and
1195 Hu, C.-G. (2022) Mobility of FLOWERING LOCUS T protein as a systemic signal in trifoliate
1196 orange and its low accumulation in grafted juvenile scions. *Horticulture Research* **9**.
1197 Xue, W., Shi, J., Li, Z., Zhang, Y., Tang, M., Du, X., An, Z., Chen, H., Yang, D. and Li, X. (2025) CmFDa-
1198 mediated epigenetic regulation of flowering in chrysanthemum. *Plant Biotechnology Journal*.
1199 Yan, X., Cao, Q.-Z., He, H.-B., Wang, L.-J. and Jia, G.-X. (2021) Functional analysis and expression
1200 patterns of members of the FLOWERING LOCUS T (FT) gene family in Lilium. *Plant Physiology*
1201 *and Biochemistry* **163**, 250-260.
1202 Zheng, R., Meng, X., Hu, Q., Yang, B., Cui, G., Li, Y., Zhang, S., Zhang, Y., Ma, X. and Song, X. (2023)
1203 OsFTL12, a member of FT-like family, modulates the heading date and plant architecture by
1204 florigen repression complex in rice. *Plant Biotechnology Journal* **21**, 1343-1360.
1205 Zhu, Y., Klasfeld, S., Jeong, C.W., Jin, R., Goto, K., Yamaguchi, N. and Wagner, D. (2020) TERMINAL
1206 FLOWER 1-FD complex target genes and competition with FLOWERING LOCUS T. *Nature*
1207 *communications* **11**, 5118.
1208 Zik, M. and Irish, V.F. (2003) Global identification of target genes regulated by APETALA3 and
1209 PISTILLATA floral homeotic gene action. *The Plant Cell* **15**, 207-222.

1210